

# MONTE CARLO GUIDED DIFFUSION FOR BAYESIAN LINEAR INVERSE PROBLEMS

GABRIEL CARDOSO, YAZID JANATI EL IDRISI, SYLVAIN LE CORFF, AND ERIC MOULINES

**ABSTRACT.** Ill-posed linear inverse problems that combine knowledge of the forward measurement model with prior models arise frequently in various applications, from computational photography to medical imaging. Recent research has focused on solving these problems with score-based generative models (SGMs) that produce perceptually plausible images, especially in inpainting problems. In this study, we exploit the particular structure of the prior defined in the SGM to formulate recovery in a Bayesian framework as a Feynman–Kac model adapted from the forward diffusion model used to construct score-based diffusion. To solve this Feynman–Kac problem, we propose the use of Sequential Monte Carlo methods. The proposed algorithm, `MCGdiff`, is shown to be theoretically grounded and we provide numerical simulations showing that it outperforms competing baselines when dealing with ill-posed inverse problems.

## 1. INTRODUCTION

This paper is concerned with linear inverse problems  $y = Ax + \sigma_y \varepsilon$ , where  $y \in \mathbb{R}_y^d$  is a vector of indirect observations,  $x \in \mathbb{R}^{d_x}$  is the vector of unknowns,  $A \in \mathbb{R}^{d_y \times d_x}$  is the linear forward operator and  $\varepsilon \in \mathbb{R}^{d_y}$  is an unknown noise vector. This general model is used throughout computational imaging, including various tomographic imaging applications such as common types of magnetic resonance imaging [Vlaardingerbroek and Boer, 2013], X-ray computed tomography [Elbakri and Fessler, 2002], radar imaging [Cheney and Borden, 2009], and basic image restoration tasks such as deblurring, superresolution, and image inpainting [González et al., 2009]. The classical approach to solving linear inverse problems relies on prior knowledge about  $x$ , such as its smoothness, sparseness in a dictionary, or its geometric properties. These approaches attempt to estimate a  $\hat{x}$  by minimizing a regularized inverse problem,  $\hat{x} = \operatorname{argmin}_x \{\|y - Ax\|^2 + \operatorname{Reg}(x)\}$ , where  $\operatorname{Reg}$  is a regularization term that balances data fidelity and noise while enabling efficient computations. However, a common difficulty in the regularized inverse problem is the selection of an appropriate regularizer, which has a decisive influence on the quality of the reconstruction.

Whereas regularized inverse problems continue to dominate the field, many alternative **statistical formulations** have been proposed; see [Besag et al., 1991, Idier, 2013, Marnissi et al., 2017] and the references therein - see also [Stuart, 2010] for a mathematical perspective. A main advantage of **statistical approaches** is that they allow for **uncertainty quantification** in the reconstructed solution; see [Dashti and Stuart, 2017]. The **Bayes' formulation** of the regularized inverse problem is based on considering the indirect measurement  $Y$ , the state  $X$  and the noise  $\varepsilon$  as random variables, and to specify  $p(y|x)$  the *likelihood* (the conditional distribution of  $Y$  at  $X$ ) and the prior  $p(x)$  (the distribution of the state). One can use Bayes' theorem to obtain the **posterior distribution**  $p(x|y) \propto p(y|x)p(x)$ , where " $\propto$ " means that the two sides are equal to each other up to a multiplicative constant that does not depend on  $x$ . Moreover, the use of an appropriate method for Bayesian inference allows the quantification of the uncertainty in the reconstructed solution  $x$ . A variety of priors are available, including but not limited to Laplace priors [Figueiredo et al., 2007], total variation (TV) priors [Kaipio et al., 2000] and mixture-of-Gaussians priors [Fergus et al., 2006]. In the last decade, a variety of techniques have been

---

Corresponding authors: [gabriel.victorino-cardoso@polytechnique.edu](mailto:gabriel.victorino-cardoso@polytechnique.edu), [yazid.janati\\_elidrissi@telecom-sudparis.eu](mailto:yazid.janati_elidrissi@telecom-sudparis.eu)

proposed to design and train generative models (GM) capable of producing perceptually realistic images [Kingma et al., 2019, Kobyzev et al., 2020, Gui et al., 2021]. Denoising diffusion models have been shown to be particularly effective generative models in this context [Sohl-Dickstein et al., 2015, Song et al., 2021c, Song et al., 2021a, Song et al., 2021b, Benton et al., 2022]. These models convert noise into natural images through a series of denoising steps. A popular approach is to use a fixed, generic diffusion model that has been pre-trained for image generation, eliminating the need for re-training and making the process more efficient and versatile [Trippe et al., 2023, Zhang et al., 2023].

Although this was not the main motivation for developing GM, these models can of course be used as prior distributions in Bayesian inverse problems. This simple observation has led to a new, fast-growing line of research on how linear inverse problems can benefit from the flexibility and expressive power of the recently introduced deep generative models; see [Arjomand Bigdeli et al., 2017, Wei et al., 2022, Su et al., 2022, Kaltenbach et al., 2023, Shin and Choi, 2023, Zhihang et al., 2023, Sahlström and Tarvainen, 2023] and the references therein.

### Contributions.

- We propose **MCGdiff**, a novel algorithm for sampling from the Bayesian posterior of Gaussian linear inverse problems with denoising diffusion model priors. **MCGdiff** specifically exploits the structure of both the linear inverse problem and the denoising diffusion generative model to design an efficient Sequential Monte Carlo (SMC) sampler.
- We establish under sensible assumptions that the empirical distribution of the samples produced by **MCGdiff** converges to the target posterior when the number of particles goes to infinity. To the best of our knowledge, **MCGdiff** is the first provably consistent algorithm for conditional sampling from the denoising diffusion posteriors.
- To evaluate the performance of **MCGdiff**, we perform numerical simulations on several examples (in high-dimension) for which the target posterior distribution is known. Simulation results support our theoretical results, i.e. the empirical distribution of samples from **MCGdiff** converges to the target posterior distribution. This is **not** the case for the competing methods (using the same denoising diffusion generative priors) which are shown, when run with random initialization of the denoising diffusion, to generate a significant number of samples outside the support of the target posterior.
- We perform experimental evaluations on inpainting problems on CelebA-HQ, showing that **MCGdiff** generates both diverse and realistic reconstructions, which are coherent with the observations.

**Background and notations.** This section provides a concise overview of the diffusion model framework and notations used in this paper. We cover only the elements that are important for understanding our approach, and we recommend that readers refer to the original papers for complete details and derivations [Sohl-Dickstein et al., 2015, Ho et al., 2020, Song et al., 2021c, Song et al., 2021a]. A denoising diffusion model is a generative model that consists of a forward and a backward process. The forward noising process involves sampling a data point  $X_0 \sim \mathbf{q}_{\text{data}}$  from the data distribution, which is then converted to a sequence  $X_{1:n}$  of recursively corrupted versions of  $X_0$ . On the other hand, the backward denoising process involves sampling  $X_n$  according to an easy-to-sample reference distribution on  $\mathbb{R}^{d_x}$  and generating  $X_0 \in \mathbb{R}^{d_x}$  by a sequence of denoising steps. Following [Sohl-Dickstein et al., 2015, Song et al., 2021a], the forward noising process can be chosen as a Markov chain with joint distribution

$$\mathbf{q}_{0:n}(x_{0:n}) = \mathbf{q}_{\text{data}}(x_0) \prod_{t=1}^n q_t(x_t | x_{t-1}), \quad q_t(x_t | x_{t-1}) = \mathcal{N}(x_t; (1 - \beta_t)^{1/2} x_{t-1}, \beta_t \mathbf{I}_{d_x}), \quad (1.1)$$

where  $\mathbf{I}_{d_x}$  is the identity matrix of size  $d_x$ ,  $\{\beta_t\}_{t \in \mathbb{N}} \subset (0, 1)$  is a non-increasing sequence and  $\mathcal{N}(\mathbf{x}; \mu, \Sigma)$  is the p.d.f. of the Gaussian distribution with mean  $\mu$  and covariance matrix  $\Sigma$  (assumed to be non-singular) evaluated at  $\mathbf{x}$ . For all  $t > 0$ , set  $\bar{\alpha}_t = \prod_{\ell=1}^t (1 - \beta_\ell)$  with the convention  $\alpha_0 = 1$ . We have for all

$0 \leq s < t \leq n$ ,

$$q_{t|s}(x_t|x_s) := \int \prod_{\ell=s+1}^t q_\ell(x_\ell|x_{\ell-1}) dx_{s+1:t-1} = \mathcal{N}(x_t; (\bar{\alpha}_t/\bar{\alpha}_s)^{1/2} x_s, (1 - \bar{\alpha}_t/\bar{\alpha}_s) \mathbf{I}_{\mathbf{d}_x}). \quad (1.2)$$

For the standard choices of  $\bar{\alpha}_t$ , the sequence of distributions  $(\mathbf{q}_t)_t$  converges weakly to the standard normal distribution as  $t \rightarrow \infty$ , which we chose as the reference distribution. For the reverse process, [Song et al., 2021a, Song et al., 2021b] introduce an *inference distribution*  $q_{1:n|0}^\sigma(x_{1:n}|x_0)$ , depending on a sequence  $\{\sigma_t\}_{t \in \mathbb{N}}$  of hyperparameters satisfying  $\sigma_t^2 \in [0, 1 - \bar{\alpha}_{t-1}]$  for all  $t \in \mathbb{N}^*$ , and defined as

$$q_{1:n|0}^\sigma(x_{1:n}|x_0) = q_{n|0}^\sigma(x_n|x_0) \prod_{t=n}^2 q_{t-1|t,0}^\sigma(x_{t-1}|x_t, x_0),$$

where  $q_{n|0}^\sigma(x_n|x_0) = \mathcal{N}(x_n; \bar{\alpha}_n^{1/2} x_0, (1 - \bar{\alpha}_n) \mathbf{I})$  and

$$q_{t-1|t,0}^\sigma(x_{t-1}|x_t, x_0) = \mathcal{N}(x_{t-1}; \boldsymbol{\mu}_t(x_0, x_t), \sigma_t^2 \mathbf{I}_d), \quad (1.3)$$

where

$$\boldsymbol{\mu}_t(x_0, x_t) = \bar{\alpha}_{t-1}^{1/2} x_0 + (1 - \bar{\alpha}_{t-1} - \sigma_t^2)^{1/2} (x_t - \bar{\alpha}_t^{1/2} x_0) / (1 - \bar{\alpha}_t)^{1/2}. \quad (1.4)$$

For  $t = n-1, \dots, 1$ , we define by backward induction the sequence:

$$q_{t|0}^\sigma(x_t|x_0) = \int q_{t|t+1,0}^\sigma(x_t|x_{t+1}, x_0) q_{t+1|0}^\sigma(x_{t+1}|x_0) dx_{t+1}. \quad (1.5)$$

It is shown in [Song et al., 2021a, Lemma 1] that for all  $t \in [1 : n]$ , the distributions of the forward and inference process conditioned on the initial state coincide, i.e. that

$$q_{t|0}^\sigma(x_t|x_0) = q_{t|0}(x_t|x_0). \quad (1.6)$$

The backward denoising process is derived from the inference distribution by replacing, for each  $t \in [2 : n]$ ,  $x_0$  in the definition  $q_{t-1|t,0}^\sigma(x_{t-1}|x_t, x_0)$  with a prediction

$$\boldsymbol{\chi}_{0|t}^\theta(x_t) := \bar{\alpha}_t^{-1/2} (x_t - (1 - \bar{\alpha}_t)^{1/2} \mathbf{e}^\theta(x_t, t)), \quad (1.7)$$

where  $\mathbf{e}^\theta(x, t)$  is typically a neural network parameterized by  $\theta$ . More formally, the backward distribution is defined as

$$\mathbf{p}_{0:n}^\theta(x_{0:n}) = \mathbf{p}_n(x_n) \prod_{t=0}^{n-1} p_t^\theta(x_t|x_{t+1}),$$

where  $\mathbf{p}_n(x_n) = \mathcal{N}(x_n; \mathbf{0}_{\mathbf{d}_x}, \mathbf{I}_{\mathbf{d}_x})$  and for all  $t \in [1 : n-1]$ ,

$$\begin{aligned} p_t^\theta(x_t|x_{t+1}) &:= q_{t|t+1,0}^\sigma(x_t|x_{t+1}, \boldsymbol{\chi}_{0|t+1}^\theta(x_{t+1})) \\ &= \mathcal{N}(x_t; \mathbf{m}_{t+1}^\theta(x_{t+1}), \sigma_{t+1}^2 \mathbf{I}_{\mathbf{d}_x}), \end{aligned} \quad (1.8)$$

where  $\mathbf{m}_{t+1}(x_{t+1}) := \boldsymbol{\mu}(\boldsymbol{\chi}_{0|t+1}^\theta(x_{t+1}), x_{t+1})$  and  $\mathbf{0}_{\mathbf{d}_x}$  is the null vector of size  $\mathbf{d}_x$ . At step 0, we set  $p_0(x_0|x_1) := \mathcal{N}(x_0; \boldsymbol{\chi}_{0|1}^\theta(x_1), \sigma_1^2 \mathbf{I}_{\mathbf{d}_x})$ . The parameter  $\theta$  is obtained (see [Song et al., 2021a, Theorem 1]) by solving the following optimization problem:

$$\theta_* \in \operatorname{argmin}_\theta \sum_{t=1}^n \frac{1}{2\mathbf{d}_x \sigma_t^2 \alpha_t} \int \|\epsilon - \mathbf{e}^\theta(\sqrt{\alpha_t} x_0 + \sqrt{1 - \alpha_t} \epsilon, t)\|_2^2 \mathcal{N}(\epsilon; \mathbf{0}_{\mathbf{d}_x}, \mathbf{I}_{\mathbf{d}_x}) \mathbf{q}_{\text{data}}(dx_0) d\epsilon. \quad (1.9)$$

Thus,  $\mathbf{e}^{\theta_*}(X_t, t)$  might be seen as the predictor of the noise added to  $X_0$  to obtain  $X_t$  (in the forward pass) and justifies the ‘‘prediction’’ terminology for (1.7). The time 0 marginal  $\mathbf{p}_0^{\theta_*}(x_0) = \int \mathbf{p}_{0:n}^{\theta_*}(x_{0:n}) dx_{1:n}$  which we will refer to as the *prior* is used as an approximation of  $\mathbf{q}_{\text{data}}$  and the time  $s$  marginal is  $\mathbf{p}_s^{\theta_*}(x_s) = \int \mathbf{p}_{0:n}^{\theta_*}(x_{0:n}) dx_{1:s-1} dx_{s+1:n}$ . In the rest of the paper we drop the dependence on the parameter  $\theta_*$ . We define for all  $v \in \mathbb{R}^\ell, w \in \mathbb{R}^k$ , the concatenation operator  $v \wedge w = [v^T, w^T]^T \in \mathbb{R}^{\ell+k}$ . For  $i \in [1 : \ell]$ , we let  $v[i]$  the  $i$ -th coordinate of the vector  $v$ .

**Related works.** The subject of Bayesian problems is very vast, and it is impossible to discuss here all the results obtained in this very rich literature. We will focus on image restoration problems, (deblurring, denoising inpainting) a challenging problem in computer vision that involves restoring a partially observed degraded image. Deep learning techniques are widely used for this task [Arjomand Bigdeli et al., 2017, Yeh et al., 2018, Xiang et al., 2023, Wei et al., 2022] with many of them relying on auto-encoders, VAEs [Ivanov et al., 2018, Peng et al., 2021, Zheng et al., 2019], GANs [Yeh et al., 2018, Zeng et al., 2022], or autoregressive transformers [Yu et al., 2018, Wan et al., 2021].

In what follows, we focus on methods based on denoising diffusion that has recently emerged as a way to produce high-quality realistic images on par with the best GANs in terms of image generation, without the intricacies of adversarial training; see [Sohl-Dickstein et al., 2015, Song et al., 2021c, Song et al., 2022]. Diffusion-based approaches do not require specific training for degradation types, making them much more versatile and computationally efficient. In [Song et al., 2022], noisy linear inverse problems are proposed to be solved by diffusing the degraded observation forward, leading to intermediate observations  $\{y_s\}_{s=0}^n$ , and then running a modified backward process that promotes consistency with  $y_s$  at each step  $s$ . The Denoising-Diffusion-Restoration model (DDRM) [Kawar et al., ] also modifies the backward process so that the unobserved part of the state follows the backward process while the observed part is obtained as a noisy weighted sum between the noisy observation and the prediction of the state. As observed by [Lugmayr et al., 2022], DDRM is very efficient, but the simple blending used occasionally causes inconsistency in the restoration process. The recently introduced DPS [Chung et al., 2023] considers a backward process targeting the posterior. DPS approximates the score of the posterior using the Tweedie formula, which incorporates the learned score of the prior. The approximation error is quantified and shown to decrease when the noise level is large, i.e., when the posterior is close to the prior distribution. As shown in Section 3 with a very simple example, neither DDRM nor DPS can be used to sample the target posterior and therefore do not solve the Bayesian recovery problem (even if we run DDRM and DPS several time with independent initializations). Indeed, we show that DDRM and DPS produce samples under the "prior" distribution (which is generally captured very well by the denoising diffusion model), but which are not consistent with the observations (many samples land in areas with very low likelihood).

In [Trippe et al., 2023] the authors introduce **SMCdiff**, a Sequential Monte Carlo-based denoising diffusion model that aims at solving specifically the *inpainting problem*. **SMCdiff** produces a particle approximation of the conditional distribution of the non observed part of the state conditionally on a forward-diffused trajectory of the observation. The resulting particle approximation is shown to converge to the true posterior of the GM under the assumption that the joint laws of the forward and backward processes coincide, which fails to be true in realistic setting. Other than being restricted to the noiseless inpainting problem, their assumption cannot be guaranteed to hold in realistic scenarios. In comparison with **SMCdiff**, **MCGdiff** is a versatile approach that solves any Bayesian linear inverse problem while being consistent under practically no assumption.

## 2. THE MCGDIFF ALGORITHM

In this section we present our methodology for the inpainting problem (2.1), both with noise and without noise. The more general case is treated in Section 2.3. Let  $d_y \in [1 : d_x - 1]$ . In what follows we may denote the  $d_y$  top coordinates of a vector  $x \in \mathbb{R}^{d_x}$  by  $\bar{x}$  and the remaining coordinates by  $\underline{x}$ , so that  $x = \bar{x} \cup \underline{x}$ . The inpainting problem is defined as

$$Y = \bar{X} + \sigma_y \varepsilon, \quad \varepsilon \sim \mathcal{N}(0, I_{d_y}), \quad \sigma \geq 0, \quad (2.1)$$

where  $\bar{X}$  are the first  $d_y$  coordinates of a random variable  $X \sim p_0$ . The goal is then to recover the law of the complete state  $X$  given a realization  $\mathbf{y}$  of the incomplete observation  $\mathbf{Y}$  and the model (2.1).

**2.1. Noiseless case.** We begin by considering the case in which  $\sigma_y = 0$ . Since the first  $d_y$  coordinates are observed exactly, we aim at inferring the remaining coordinates of the random variable, which

correspond to  $\underline{X}$ . As such, given an observation  $y$ , we aim at sampling from the posterior given by  $\phi_0^y(\underline{x}_0) \propto p_0(y \cap \underline{x}_0)$  and which has integral form

$$\phi_0^y(\underline{x}_0) \propto \int p_n(x_n) \left\{ \prod_{s=1}^{n-1} p_s(x_s | x_{s+1}) \right\} p_0(y \cap \underline{x}_0 | x_1) dx_{1:n}. \quad (2.2)$$

To solve this problem, we propose to use Sequential Monte Carlo (SMC) algorithms [Doucet et al., 2001, Cappé et al., 2005, Chopin et al., 2020], where a set of  $N$  random samples, referred to as particles, is iteratively updated to approximate the posterior distribution. The updates involve, at iteration  $s$ , selecting promising particles from  $\xi_{s+1}^{1:N} = (\xi_{s+1}^1, \dots, \xi_{s+1}^N)$  based on a weight function  $\tilde{\omega}_s$ , to which we then apply a Markov transition  $p_s^y$  to obtain the samples  $\xi_s^{1:N}$ . The transition  $p_s^y(x_s | x_{s+1})$  is designed to follow the backward process while guiding the  $\mathbf{d}_y$  top coordinates of the pool of particles  $\xi_s^{1:N}$  towards the measurement  $y$ . Before we proceed to define the transition kernels, note that under the backward dynamics (1.8),  $\bar{X}_t$  and  $\underline{X}_t$  are independent conditionally on  $X_{t+1}$  with transition kernels respectively

$$\bar{p}_t(\bar{x}_t | x_{t+1}) := \mathcal{N}(\bar{x}_t; \bar{\mathbf{m}}_{t+1}(x_{t+1}), \sigma_{t+1}^2 \mathbf{I}_{\mathbf{d}_y}), \quad \underline{p}_t(\underline{x}_t | x_{t+1}) := \mathcal{N}(\underline{x}_t; \underline{\mathbf{m}}_{t+1}(x_{t+1}), \sigma_{t+1}^2 \mathbf{I}_{\mathbf{d}_x - \mathbf{d}_y})$$

where  $\bar{\mathbf{m}}_{t+1}(x_{t+1}) \in \mathbb{R}^{\mathbf{d}_y}$  and  $\underline{\mathbf{m}}_{t+1}(x_{t+1}) \in \mathbb{R}^{\mathbf{d}_x - \mathbf{d}_y}$  are such that  $\mathbf{m}_{t+1}(x_{t+1}) = \bar{\mathbf{m}}_{t+1}(x_{t+1}) \cap \underline{\mathbf{m}}_{t+1}(x_{t+1})$  and the above kernels satisfy  $p_t(x_s | x_{s+1}) = \bar{p}_t(\bar{x}_t | x_{t+1}) \underline{p}_t(\underline{x}_t | x_{t+1})$ .

We consider the following proposal kernels for the steps  $t \in [1 : n]$ ,

$$p_s^y(x_t | x_{t+1}) \propto p_t(x_t | x_{t+1}) \bar{q}_{t|0}(\bar{x}_t | y), \quad \text{where } \bar{q}_{t|0}(\bar{x}_t | y) := \mathcal{N}(\bar{x}_t; \bar{\alpha}_t^{1/2} y, (1 - \bar{\alpha}_t) \mathbf{I}_{\mathbf{d}_y}), \quad (2.3)$$

and  $p_n^y(x_n) \propto p_n(x_n) \bar{q}_{n|0}(\bar{x}_n | y)$ . For the final step, we use the kernel  $\underline{p}_0^y(\underline{x}_0 | x_1) = \underline{p}_0(\underline{x}_0 | x_1)$ . Using standard Gaussian conjugation formulas, we find that

$$\begin{aligned} p_t^y(x_t | x_{t+1}) &= \underline{p}_t(\underline{x}_t | x_{t+1}) \cdot \mathcal{N}(\bar{x}_t; \mathbf{K}_t \alpha_t^{1/2} y + (1 - \mathbf{K}_t) \bar{\mathbf{m}}_{t+1}(x_{t+1}), (1 - \bar{\alpha}_t) \mathbf{K}_t \cdot \mathbf{I}_{\mathbf{d}_y}), \\ p_n(x_n) &= \mathcal{N}(\underline{x}_n; \mathbf{0}_{\mathbf{d}_x - \mathbf{d}_y}, \mathbf{I}_{\mathbf{d}_x - \mathbf{d}_y}) \cdot \mathcal{N}(\bar{x}_n; \mathbf{K}_n \bar{\alpha}_n^{1/2} y, (1 - \bar{\alpha}_n) \mathbf{K}_n \cdot \mathbf{I}_{\mathbf{d}_y}) \end{aligned}$$

where  $\mathbf{K}_t := \sigma_{t+1}^2 / (\sigma_{t+1}^2 + 1 - \alpha_t)$ . For this procedure to target the posterior  $\phi_0^y$ , the weight function  $\tilde{\omega}_s$  is chosen as follows; we set

$$\begin{aligned} \tilde{\omega}_{n-1}(x_n) &:= \int p_{n-1}(x_{n-1} | x_n) \bar{q}_{n-1|0}(\bar{x}_{n-1} | y) dx_{n-1} \\ &= \mathcal{N}(\alpha_{n-1}^{1/2} y; \bar{\mathbf{m}}_n(x_n), \sigma_n^2 + 1 - \alpha_s) \end{aligned}$$

and for  $t \in [1 : n - 2]$ ,

$$\begin{aligned} \tilde{\omega}_t(x_{t+1}) &:= \int \bar{p}_t(\bar{x}_t | x_{t+1}) \bar{q}_{t|0}(\bar{x}_t | y) dx_t / \bar{q}_{t+1|0}(\bar{x}_{t+1} | y) \\ &= \frac{\mathcal{N}(\alpha_t^{1/2} y; \bar{\mathbf{m}}_{t+1}(x_{t+1}), (\sigma_{t+1}^2 + 1 - \alpha_t) \mathbf{I}_{\mathbf{d}_y})}{\mathcal{N}(\alpha_{t+1}^{1/2} y; \bar{x}_{t+1}, (1 - \alpha_{t+1}) \mathbf{I}_{\mathbf{d}_y})}. \end{aligned} \quad (2.4)$$

For the final step, we set  $\tilde{\omega}_0(x_1) := \bar{p}_0(y | \bar{x}_1) / \bar{q}_{1|0}(\bar{x}_1 | y)$ . The overall SMC algorithm targeting  $\phi_0^y$  using the instrumental kernel (2.3) and weight function (2.4) is summarized in Algorithm 1.

We now provide a justification to Algorithm 1. Let  $\{g_s^y\}_{s=1}^n$  be a sequence of positive functions. Consider the sequence of distributions  $\{\phi_s^y\}_{s=1}^n$  defined as follows;  $\phi_s^y(x_n) \propto p_n(x_n) g_n^y(x_n)$  and for  $t \in [1 : n - 1]$

$$\phi_t^y(x_t) \propto \int \frac{g_t^y(x_t)}{g_{t+1}^y(x_{t+1})} p_t(x_t | x_{t+1}) \phi_{t+1}^y(dx_{t+1}), \quad (2.5)$$

**Algorithm 1:** MCGdiff ( $\sigma = 0$ )

---

**Input:** Number of particles  $N$   
**Output:**  $\xi_0^{1:N}$

// Operations involving index  $i$  are repeated for each  $i \in [1 : N]$

$\bar{z}_n^i \sim \mathcal{N}(\mathbf{0}_{d_y}, \mathbf{I}_{d_y}), \quad z_n^i \sim \mathcal{N}(\mathbf{0}_{d_x-d_y}, \mathbf{I}_{d_x-d_y});$   
 $\bar{\xi}_n^i = \mathbf{K}_n \bar{\alpha}_n^{1/2} y + (1 - \bar{\alpha}_n) \mathbf{K}_n \bar{z}_n^i;$   
Set  $\xi_n^i = \bar{\xi}_n^i \bar{z}_n^i;$   
**for**  $s \leftarrow n - 1 : 0$  **do**  
  **if**  $s = n - 1$  **then**  
     $\tilde{\omega}_{n-1}(\xi_n^i) = \mathcal{N}(\bar{\alpha}_n^{1/2} y; \bar{m}_n(\xi_n^i), 2 - \bar{\alpha}_n);$   
  **else**  
     $\tilde{\omega}_s(\xi_{s+1}^i) = \mathcal{N}(\bar{\alpha}_s^{1/2} y; \bar{m}_{s+1}(\xi_{s+1}^i), \sigma_{s+1}^2 + 1 - \bar{\alpha}_s) / \mathcal{N}(\bar{\alpha}_{s+1}^{1/2} y; \bar{\xi}_{s+1}^i, 1 - \bar{\alpha}_{s+1});$   
     $I_{s+1}^i \sim \text{Categorical}(\{\tilde{\omega}_s(\xi_{s+1}^j) / \sum_{k=1}^N \tilde{\omega}_s(\xi_{s+1}^k)\}_{j=1}^N);$   
     $\bar{z}_s^i \sim \mathcal{N}(\mathbf{0}_{d_y}, \mathbf{I}_{d_y}), \quad z_s^i \sim \mathcal{N}(\mathbf{0}_{d_x-d_y}, \mathbf{I}_{d_x-d_y});$   
     $\bar{\xi}_s^i = \mathbf{K}_s \bar{\alpha}_s^{1/2} y + (1 - \mathbf{K}_s) \bar{m}_{s+1}(\xi_{s+1}^i) + (1 - \alpha_s)^{1/2} \mathbf{K}_s^{1/2} \bar{z}_s^i;$   
     $\underline{\xi}_s^i = \underline{m}_{s+1}(\xi_{s+1}^i) + \sigma_{s+1} z_s^i;$   
    Set  $\xi_s^i = \bar{\xi}_s^i \bar{z}_s^i;$

---

By construction, the time  $t$  marginal (2.5) is  $\phi_t^y(x_t) \propto p_t(x_t) g_t^y(x_t)$  for all  $t \in [1 : n]$ . Then, using  $\phi_1^y$  and (2.2), we have that

$$\phi_0^y(x_0) \propto \int \frac{\bar{p}_0(y|\bar{x}_1)}{g_1^y(x_1)} \underline{p}_0(x_0|x_1) \phi_1^y(dx_1). \quad (2.6)$$

The recursion (2.5) suggests a way of obtaining a particle approximation of  $\phi_0^y$ ; by sequentially approximating each  $\phi_t^y$  we can effectively derive a particle approximation of the posterior using (2.6). To construct the intermediate particle approximations we use the framework of *auxiliary particle filters* (APF) [Pitt and Shephard, 1999]. We focus on the particular case where  $g_t^y(x_t) = \bar{q}_{t|0}(\bar{x}_t|y)$  which corresponds to Algorithm 1. The initial particle approximation  $\phi_0^y$  is obtained by drawing  $N$  i.i.d. samples  $(\xi_n^1, \dots, \xi_n^N)$  from  $p_n^y$  and setting  $\phi_n^N = N^{-1} \sum_{i=1}^N \delta_{\xi_n^i}$  where  $\delta_\xi$  is the Dirac mass at  $\xi$ . Assume that the empirical approximation of  $\phi_{t+1}^y$  is

$$\phi_{t+1}^N = N^{-1} \sum_{i=1}^N \delta_{\xi_{t+1}^i},$$

where  $(\xi_{t+1}^1, \dots, \xi_{t+1}^N)$  are  $N$  random variables. Substituting  $\phi_{t+1}^N$  into the recursion (2.5) and introducing the instrumental kernel (2.3), we obtain the following mixture

$$\hat{\phi}_t^N(x_t) = \sum_{i=1}^N \frac{\tilde{\omega}_t(\xi_{t+1}^i)}{\sum_{j=1}^N \tilde{\omega}_t(\xi_{t+1}^j)} p_t^y(x_t|\xi_{t+1}^i). \quad (2.7)$$

Then, a particle approximation of (2.7) is obtained by sampling  $N$  conditionally i.i.d. ancestor indices

$$I_{t+1}^{1:N} \stackrel{\text{i.i.d.}}{\sim} \text{Categorical}(\{\tilde{\omega}_t(\xi_{t+1}^i) / \sum_{j=1}^N \tilde{\omega}_t(\xi_{t+1}^j)\}_{i=1}^N)$$

and then propagating each ancestor particle  $\xi_{s+1}^{I_{t+1}^i}$  according to the instrumental kernel (2.3). The final particle approximation is given by

$$\phi_0^N = N^{-1} \sum_{i=1}^N \delta_{\xi_0^i}, \quad \text{where } \xi_0^i \sim p_0(\cdot | \xi_1^{I_0^i}), \quad I_0^i \sim \text{Categorical}(\{\tilde{\omega}_0(\xi_1^k) / \sum_{j=1}^N \tilde{\omega}_0(\xi_1^j)\}_{k=1}^N).$$

The potential  $g_t^y(x_t) = \bar{q}_{t|0}(\bar{x}_t | y)$ , and hence Equations (2.5) and (2.6), is motivated by considering the posterior of the state under the forward process (1.1)  $\rho_t^y(x_t) := \int \phi_0^y(\underline{x}_0) q_{t|0}(x_t | y \setminus \underline{x}_0) d\underline{x}_0$ . Indeed, first note that the bridge kernel decomposes across the dimensions as follows,

$$q_{t-1|t,0}^\sigma(x_{t-1} | x_t, x_0) = \bar{q}_{t-1|t,0}^\sigma(\bar{x}_{t-1} | \bar{x}_t, \bar{x}_0) \underline{q}_{t-1|t,0}^\sigma(x_{t-1} | \underline{x}_t, \underline{x}_0)$$

where

$$\begin{aligned} \bar{q}_{t|t+1,0}^\sigma(\bar{x}_t | \bar{x}_{t+1}, \bar{x}_0) &= \mathcal{N}(\bar{x}_t; \boldsymbol{\mu}_t(\bar{x}_0, \bar{x}_{t+1}), \sigma_{t+1}^2 \mathbf{I}_{\mathbf{d}_y}), \\ \underline{q}_{t-1|t,0}^\sigma(x_{t-1} | \underline{x}_t, \underline{x}_0) &= \mathcal{N}(x_{t-1}; \boldsymbol{\mu}_t(\underline{x}_0, \underline{x}_t), \sigma_t^2 \mathbf{I}_{\mathbf{d}_x - \mathbf{d}_y}), \end{aligned}$$

and  $\boldsymbol{\mu}_{t+1}$  is defined in (1.4). It is then easily seen that

$$\begin{aligned} \bar{q}_{t|0}(\bar{x}_t | \bar{x}_0) &= \int \bar{q}_{t|t+1,0}^\sigma(\bar{x}_t | \bar{x}_{t+1}, \bar{x}_0) \bar{q}_{t+1|0}(d\bar{x}_{t+1} | \bar{x}_0) \\ \underline{q}_{t|0}(\underline{x}_t | \underline{x}_0) &= \int \underline{q}_{t|t+1,0}^\sigma(x_t | \underline{x}_{t+1}, \underline{x}_0) \underline{q}_{t+1|0}(dx_{t+1} | \underline{x}_0), \end{aligned}$$

where  $\underline{q}_{t|0}$  is defined analogously to  $\bar{q}_{t|0}$  in (2.3). Hence, using that  $q_{t|0}(x_t | x_0) = \bar{q}_{t|0}(\bar{x}_t | \bar{x}_0) \underline{q}_{t|0}(\underline{x}_t | \underline{x}_0)$ , we see that

$$\begin{aligned} \rho_t^y(x_t) &= \int \phi_0^y(d\underline{x}_0) \bar{q}_{t|0}(\bar{x}_t | y) \underline{q}_{t|t+1,0}^\sigma(x_t | \underline{x}_{t+1}, \underline{x}_0) \bar{q}_{t+1|0}(d\underline{x}_{t+1} | \underline{x}_0) \\ &= \int \phi_0^y(d\underline{x}_0) \bar{q}_{t|0}(\bar{x}_t | y) \underline{q}_{t|t+1,0}^\sigma(x_t | \underline{x}_{t+1}, \underline{x}_0) q_{t+1|0}(dx_{t+1} | y \setminus x_0). \end{aligned}$$

Finally, replacing  $\underline{x}_0$  by the vector made of the last  $\mathbf{d}_x - \mathbf{d}_y$  coordinates of its prediction  $\boldsymbol{\chi}_{0|s+1}(x_{s+1})$ , which we denote by  $\boldsymbol{\chi}_{0|s+1}(x_{s+1})$ , we see that  $\rho_s^y$  satisfies

$$\rho_s^y(x_s) \approx \int \bar{q}_{s|0}(\bar{x}_s | y) p_s(\underline{x}_s | x_{s+1}) \rho_{s+1}^y(dx_{s+1}). \quad (2.8)$$

According to this recursion, the transition from  $\underline{x}_s$  should follow the backward process conditioned by  $x_{s+1}$ , while that from  $\bar{x}_s$  should follow the forward one conditioned on the measurement  $y$  at time 0. Equation (2.5) reflects this behaviour, while (2.6) ensures that the procedure ultimately produces the posterior as the final marginal. The idea of using the forward diffused observation to guide the observed part of the state, as we do here through  $\bar{q}_t(\bar{x}_t | y)$ , has been exploited in prior works but in a different way. For instance, in [Song et al., 2021c, Song et al., 2022] the observed part of the state is directly replaced by the forward noisy observation and, as it has been noted [Trippe et al., 2023], this introduces an irreducible error resulting in a procedure that fails to sample from the posterior. Instead, **MCGdiff** weights the backward process by the density of the forward one conditioned on  $y$ , resulting in a natural and consistent algorithm.

We now establish the convergence of **MCGdiff** with a general sequence of potentials  $\{g_s^y\}_{s=1}^n$ . We consider the following assumption on the sequence of potentials  $\{g_t^y\}_{t=1}^n$ .

$$(\mathbf{A1}) \quad (\text{i}) \quad \sup_{x_1 \in \mathbb{R}^{\mathbf{d}_x}} \bar{p}_0(y | x_1) / g_1^y(x_1) < \infty,$$

$$(\text{ii}) \quad \sup_{x_{t+1} \in \mathbb{R}^{\mathbf{d}_x}} \int g_t^y(x_t) p_t(x_t | x_{t+1}) dx_t / g_{t+1}^y(x_{t+1}) < \infty \text{ for all } t \in [1 : n-1].$$

The following exponential deviation inequality is standard and is a direct application of [Douc et al., 2014, Theorem 10.17]. In particular, it implies a  $\mathcal{O}(1/\sqrt{N})$  bound on the mean squared error  $\|\phi_0^N(h) - \phi_0^y(h)\|_2$ .

**Proposition 2.1.** *Assume (A1). There exist constants  $c_{1,n}, c_{2,n} \in (0, \infty)$  such that, for all  $N \in \mathbb{N}$ ,  $\varepsilon > 0$  and bounded function  $h : \mathbb{R}^{\mathbf{d}_x} \mapsto \mathbb{R}$ ,*

$$\mathbb{P} [|\phi_0^N(h) - \phi_0^y(h)| \geq \varepsilon] \leq c_{1,n} \exp(-c_{2,n} N \varepsilon^2 / \|h\|_\infty^2)$$

where  $\|h\|_\infty := \sup_{x \in \mathbb{R}^{\mathbf{d}_x}} |h(x)|$ .

We also furnish our estimator with an explicit non-asymptotic bound on its bias. Define  $\Phi_0^N = \mathbb{E}[\phi_0^N]$  where  $\phi_0^N = N^{-1} \sum_{i=1}^N \delta_{\xi_0^i}$  is the particle approximation produced by Algorithm 1 and the expectation is with respect to the law of  $(\xi_0^{1:N}, \dots, \xi_n^{1:N}, I_0^{1:N}, \dots, I_{n-1}^{1:N})$ . Define for all  $t \in [1 : n]$ ,

$$\phi_t^*(x_t) \propto \mathbf{p}_t(x_t) \int \delta_y(d\bar{x}_0) p_{0|t}(x_0|x_t) d\bar{x}_0,$$

where  $p_{0|t}(x_0|x_t) := \int \left\{ \prod_{s=0}^{t-1} p_s(x_s|x_{s+1}) \right\} dx_{1:t-1}$ .

**Proposition 2.2.** *It holds that*

$$\mathsf{KL}(\phi_0^y \parallel \Phi_0^N) \leq \frac{C_{0:n}^y}{N-1} + \frac{D_{0:n}^y}{N^2}, \quad (2.9)$$

where  $D_{0:n}^y > 0$ ,

$$C_{0:n}^y := \sum_{t=1}^n \int \frac{\mathcal{Z}_t / \mathcal{Z}_0}{g_t^y(z_t)} \left\{ \int \delta_y(d\bar{x}_0) p_{0|t}(x_0|z_t) d\bar{x}_0 \right\} \phi_t^*(dz_t), \quad (2.10)$$

and  $\mathcal{Z}_t := \int g_t^y(x_t) \mathbf{p}_t(dx_t)$  for all  $t \in [1 : n]$  and  $\mathcal{Z}_0 := \int \delta_y(d\bar{x}_0) \mathbf{p}_0(x_0) d\bar{x}_0$ . If furthermore (A1) holds then both  $C_{0:n}^y$  and  $D_{0:n}^y$  are finite.

The proof of Proposition 2.2 is postponed to Appendix B.1. (A1) is an assumption on the equivalent of the weights  $\{\tilde{w}_t\}_{t=0}^n$  with a general sequence of potentials  $\{g_s^y\}_{s=1}^n$  and is not restrictive as it can be satisfied by setting for example  $g_s^y(x_s) = \bar{q}_{s|0}(\bar{x}_s|y) + \delta$  where  $\delta > 0$ . The resulting algorithm is then only a slight modification of the one described above, see Appendix B.1 for more details. It is also worth noting that Proposition 2.2 combined with Pinsker's inequality implies that the bias of **MCGdiff** goes to 0 with the number of particle samples  $N$  for fixed  $n$ . We have chosen to present a bound in Kullback–Leibler (KL) divergence, inspired by [Andrieu et al., 2018, Huggins and Roy, 2019], as it allows an explicit dependence on the modeling choice  $\{g_s^y\}_{s=1}^n$ , see Lemma B.2. Finally, unlike the theoretical guarantees established for **SMCdiff** in [Trippe et al., 2023], proving the asymptotic exactness of our methodology w.r.t. to the generative model posterior does not require having  $\mathbf{p}_{s+1}(x_{s+1})p_s(x_s|x_{s+1}) = \mathbf{p}_s(x_s)q_{s+1}(x_{s+1}|x_s)$  for all  $s \in [0 : n - 1]$ , i.e. that the one step forward kernel is the time reversal of the backward one, which does not in hold in practice. As such, **SMCdiff** exhibits a non-vanishing asymptotic bias.

**2.2. Noisy case.** We now turn to the case  $\sigma_y > 0$ . The posterior density we consider in this section is given by

$$\phi_0^y(x_0) \propto g_0^y(\bar{x}_0) \mathbf{p}_0(x_0), \quad \text{where } g_0^y : x_0 \mapsto \mathcal{N}(y; \bar{x}_0, \sigma_y^2 \mathbf{I}_{\mathbf{d}_y}). \quad (2.11)$$

In what follows we assume that there exists a timestep  $\tau \in [1 : n]$  such that  $\sigma^2 = (1 - \bar{\alpha}_\tau) / \bar{\alpha}_\tau$ . We discuss this assumption in the numerical section. In what follows we denote  $\tilde{y}_\tau = \bar{\alpha}_\tau^{1/2} y$ . We can then write that

$$\begin{aligned} g_0^y(\bar{x}_0) &= \bar{\alpha}_\tau^{1/2} \cdot \mathcal{N}(\tilde{y}_\tau; \bar{\alpha}_\tau^{1/2} x_0, (1 - \bar{\alpha}_\tau) \cdot \mathbf{I}_{\mathbf{d}_y}) \\ &= \bar{\alpha}_\tau^{1/2} \cdot \bar{q}_{\tau|0}(\tilde{y}_\tau | \bar{x}_0), \end{aligned} \quad (2.12)$$

which hints that the likelihood function  $g_0^y$  is closely related to the forward process (1.1). We may then write the posterior (2.11) as follows

$$\begin{aligned}\phi_0^y(x_0) &\propto \int \delta_{\tilde{y}_\tau}(\mathrm{d}\bar{x}_s) \bar{q}_{\tau|0}(\bar{x}_\tau|\bar{x}_0) \mathbf{p}_0(x_0) \\ &\propto \int \delta_{\tilde{y}_\tau}(\mathrm{d}\bar{x}_\tau) q_{\tau|0}(x_\tau|x_0) \mathbf{p}_0(x_0) \mathrm{d}\underline{x}_\tau,\end{aligned}$$

Next, let us assume that the forward process (1.1) is the reverse of the backward one (1.8), i.e. that

$$\mathbf{p}_t(x_t) q_{t+1}(x_{t+1}|x_t) = \mathbf{p}_{t+1}(x_{t+1}) p_t(x_t|x_{t+1}), \quad \forall t \in [0 : n-1]. \quad (2.13)$$

This is similar to the assumption made in **SMCdiff** [Trippe et al., 2023]. Then, it is easily seen that it implies  $\mathbf{p}_0(x_0) q_{\tau|0}(x_\tau|x_0) = \mathbf{p}_\tau(x_\tau) p_{0|\tau}(x_0|x_\tau)$  and thus

$$\begin{aligned}\phi_0^y(x_0) &= \frac{\int p_{0|\tau}(x_0|x_\tau) \delta_{\tilde{y}_\tau}(\mathrm{d}\bar{x}_\tau) \mathbf{p}_\tau(x_\tau) \mathrm{d}\underline{x}_\tau}{\int \delta_{\tilde{y}_\tau}(\mathrm{d}\bar{z}_\tau) \mathbf{p}_\tau(z_\tau) \mathrm{d}\underline{z}_\tau} \\ &= \int p_{0|\tau}(x_0|\tilde{y}_\tau \underline{x}_\tau) \phi_\tau^{\tilde{y}_\tau}(\mathrm{d}x_\tau),\end{aligned} \quad (2.14)$$

where  $\phi_\tau^{\tilde{y}_\tau}(\underline{x}_\tau) \propto \mathbf{p}_\tau(\tilde{y}_\tau \underline{x}_\tau)$ . (2.14) highlights that solving the inverse problem (2.1) with  $\sigma_y > 0$  is equivalent to solving an inverse problem on the intermediate state  $X_\tau \sim \mathbf{p}_\tau$  with *noiseless* observation  $\tilde{y}_\tau$  of the  $\mathbf{d}_y$  top coordinates and then propagating the resulting posterior back to time 0 with the backward kernel  $p_{0|\tau}$ . To obtain a particle approximation of  $\phi_\tau^{\tilde{y}_\tau}$  we may then use the methodology of the previous section with the potentials  $g_t^y : x_t \mapsto \bar{q}_{t|\tau}(x_t|\tilde{y}_\tau)$  for  $t \in [\tau+1 : n]$ . Indeed, consider the sequence  $\{\rho_t^{\tilde{y}_\tau}\}_{t=\tau}^n$  defined by  $\rho_t^{\tilde{y}_\tau}(x_t) = \int \phi_\tau^{\tilde{y}_\tau}(\mathrm{d}x_\tau) q_{t|\tau}(x_t|\tilde{y}_\tau \underline{x}_\tau)$ . Using that  $\mathbf{p}_\tau(x_\tau) = \int \mathbf{p}_0(\mathrm{d}x_0) q_{\tau|0}(x_\tau|x_0)$  by assumption and the identity (1.5), we find that

$$\begin{aligned}\rho_t^{\tilde{y}_\tau}(x_t) &\propto \int \mathbf{p}_0(\mathrm{d}x_0) \bar{q}_{\tau|0}(\tilde{y}_\tau|\bar{x}_0) \bar{q}_{t|\tau}(\bar{x}_t|\tilde{y}_\tau) q_{t|0}(x_t|\underline{x}_0) \\ &\propto \int \mathbf{p}_0(\mathrm{d}x_0) \bar{q}_{\tau|0}(\tilde{y}_\tau|\bar{x}_0) \bar{q}_{t|\tau}(\bar{x}_t|\tilde{y}_\tau) \bar{q}_{t+1|\tau}(\mathrm{d}\bar{x}_{t+1}|\tilde{y}_\tau) q_{t+1,0}^\sigma(\underline{x}_t|\underline{x}_{t+1}, \underline{x}_0) q_{t+1|0}(\mathrm{d}\underline{x}_{t+1}|\underline{x}_0),\end{aligned}$$

and replacing  $\underline{x}_0$  in the bridge kernel  $q_{t|t+1,0}^\sigma$  by  $\underline{\chi}_{0|s+1}(x_{s+1})$ , we obtain the recursion

$$\rho_t^{\tilde{y}_\tau}(x_t) \approx \int \bar{q}_{t|\tau}(\bar{x}_t|\tilde{y}_\tau) \underline{\mathbf{p}}_t(\underline{x}_t|x_{t+1}) \rho_{t+1}^{\tilde{y}_\tau}(\mathrm{d}x_{t+1}), \quad (2.15)$$

which provides the intuition for our choice of potential.

The assumption (2.13) regarding the reversal of the backward process holds only approximately in realistic settings. Therefore, while (2.14) also holds only approximately in practice, we can still use it as inspiration for designing potentials when the assumption is not valid. Consider then  $\{g_t^y\}_{t=\tau}^n$  and sequence of probability measures  $\{\phi_t^y\}_{t=\tau}^n$  defined for all  $t \in [\tau : n]$  as

$$\phi_t^y(x_t) \propto g_t^y(x_t) \mathbf{p}_t(x_t), \quad \text{where } g_t^y : x_t \mapsto \mathcal{N}(x_t; \tilde{y}_\tau, (1 - (1 - \kappa)\bar{\alpha}_t/\bar{\alpha}_\tau) \mathbf{I}_{\mathbf{d}_y}), \quad \kappa \geq 0. \quad (2.16)$$

In the particular case of  $\kappa = 0$ , we have that  $g_t^y(x_t) = \bar{q}_{t|\tau}(\bar{x}_t|\tilde{y}_\tau)$  for  $t \in [\tau+1 : n]$  and  $\phi_\tau^y = \phi_\tau^{\tilde{y}_\tau}$ . The recursion (2.5) holds for  $t \in [\tau : n]$  and assuming that  $\kappa > 0$ , we find that

$$\phi_0^y(x_0) \propto \int \frac{g_0^y(x_0)}{g_\tau^y(x_\tau)} p_{0|\tau}(x_0|x_\tau) \phi_\tau^y(\mathrm{d}x_\tau),$$

which resembles the recursion (2.14). In practice we take  $\kappa$  to be small in order to mimick the Dirac delta mass at  $\bar{x}_\tau$  in (2.14). Having obtained a particle approximation  $\phi_\tau^N = N^{-1} \sum_{i=1}^N \delta_{\xi_\tau^i}$  of  $\phi_\tau^y$  by adapting Algorithm 1, we estimate  $\phi_0^y$  with

$$\phi_0^N = \sum_{i=1}^N \omega_0^i \delta_{\xi_0^i}, \quad \text{where } \xi_0^i \sim p_{0|\tau}(\cdot|\xi_\tau^i), \quad \omega_0^i = \frac{g_0^y(\xi_0^i)/g_\tau^y(\xi_\tau^i)}{\sum_{j=1}^N g_0^y(\xi_0^j)/g_\tau^y(\xi_\tau^j)}.$$

In the next section we extend this methodology to general linear Gaussian observation models. Finally, note that (2.14) allows us to extend **SMCdiff** to handle noisy inverse problems in a principled manner. This is detailed in Appendix A.

**2.3. Extension to general linear inverse problems.** We now extend **MCGdiff** to a general linear Gaussian observation model. Consider  $Y = AX + \sigma_y \varepsilon$  where  $A \in \mathbb{R}^{d_y \times d_x}$ ,  $\varepsilon \sim \mathcal{N}(0_{d_y}, I_{d_y})$  and  $\sigma_y \geq 0$  and the singular value decomposition (SVD)  $A = US\bar{V}^T$ , where  $\bar{V} \in \mathbb{R}^{d_x \times d_y}$ ,  $U \in \mathbb{R}^{d_y \times d_y}$  are two orthonormal matrices, and  $S \in \mathbb{R}^{d_y \times d_y}$  is diagonal. For simplicity, it is assumed that the singular values are all distinct  $s_1 > s_2 > \dots > s_{d_y} > 0$ . Set  $b = d_x - d_y$ . Let  $\underline{V} \in \mathbb{R}^{d_x \times b}$  be an orthonormal matrix of which the columns complete those of  $\bar{V}$  into an orthonormal basis of  $\mathbb{R}^{d_x}$ , i.e.  $\underline{V}^T \underline{V} = I_b$  and  $\underline{V}^T \bar{V} = \mathbf{0}_{b, d_y}$ . We define  $V = [\bar{V}, \underline{V}] \in \mathbb{R}^{d_x \times d_x}$ . In what follows, for a given  $\mathbf{x} \in \mathbb{R}^{d_x}$  we write  $\bar{\mathbf{x}} \in \mathbb{R}^{d_y}$  for its top  $d_y$  coordinates and  $\underline{\mathbf{x}} \in \mathbb{R}^b$  for the remaining coordinates. Multiplying the measurement equation by  $S^{-1}U^T$  yields

$$\mathbf{Y} = \bar{\mathbf{X}} + \sigma_y S^{-1} \tilde{\varepsilon}, \quad \tilde{\varepsilon} \sim \mathcal{N}(0, I_{d_y}),$$

where  $\mathbf{X} := V^T X$  and  $\mathbf{Y} := S^{-1}U^T Y$ . In this section, we focus on solving this linear inverse problem in the orthonormal basis defined by  $V$  using the methodology developed in the previous sections. This prompts us to define the diffusion based generative model in this basis. As  $V$  is an orthonormal matrix, the law of  $\mathbf{X}_0 = V^T X_0$  is  $\mathbf{p}_0(\mathbf{x}_0) := \mathbf{p}_0(V\mathbf{x}_0)$ . By definition of  $\mathbf{p}_0$  and the fact that  $\|V\mathbf{x}\|_2 = \|\mathbf{x}\|_2$  for all  $\mathbf{x} \in \mathbb{R}^{d_x}$  we have that

$$\begin{aligned} \mathbf{p}_0(\mathbf{x}_0) &= \int p_0(V\mathbf{x}_0 | \mathbf{x}_1) \left\{ \prod_{s=1}^{n-1} p_s(d\mathbf{x}_s | \mathbf{x}_{s+1}) \right\} \mathbf{p}_n(d\mathbf{x}_n) \\ &= \int \lambda_0(\mathbf{x}_0 | \mathbf{x}_1) \left\{ \prod_{s=1}^{n-1} \lambda_s(d\mathbf{x}_s | \mathbf{x}_{s+1}) \right\} \mathbf{p}_n(d\mathbf{x}_n) \end{aligned}$$

where for all  $s \in [0 : n - 1]$ ,

$$\lambda_s(\mathbf{x}_s | \mathbf{x}_{s+1}) := \mathcal{N}(\mathbf{x}_s; \mathbf{m}_{s+1}(\mathbf{x}_{s+1}), \sigma_{s+1}^2 I_{d_x}), \quad \text{where } \mathbf{m}_{s+1}(\mathbf{x}_{s+1}) := V^T \mathbf{m}_{s+1}(V\mathbf{x}_{s+1}).$$

The transition kernels  $\{\lambda_s\}_{s=0}^n$  thus define a diffusion based model in the basis  $V$ . In the following we shall write  $\bar{\mathbf{m}}_{s+1}(\mathbf{x}_{s+1})$  for the first  $d_y$  coordinates of  $\mathbf{m}_{s+1}(\mathbf{x}_{s+1})$  and  $\underline{\mathbf{m}}_{s+1}(\mathbf{x}_{s+1})$  the last  $b$  coordinates. We denote by  $\mathbf{p}_s$  the time  $s$  marginal of the backward process,

*Noiseless.* In this case the target posterior is  $\phi_0^{\mathbf{y}}(\mathbf{x}_0) \propto \mathbf{p}_0(\mathbf{y}^\frown \underline{\mathbf{x}}_0)$ . The extension of the algorithm described in section 2.1 is thus straightforward; it is enough to replace  $y$  with  $\mathbf{y}$  ( $= S^{-1}U^T y$ ) and the backward kernels  $\{p_t\}_{t=0}^{n-1}$  with  $\{\lambda_t\}_{t=0}^{n-1}$ .

*Noisy.* The posterior density is then

$$\phi_0^{\mathbf{y}}(\mathbf{x}_0) \propto g_0^{\mathbf{y}}(\bar{\mathbf{x}}_0) \mathbf{p}_0(\mathbf{x}_0), \quad \text{where } g_0^{\mathbf{y}}(\bar{\mathbf{x}}_0) = \prod_{i=1}^{d_y} \mathcal{N}(\mathbf{y}[i]; \bar{\mathbf{x}}_0[i], (\sigma_y/s_i)^2).$$

We now generalize Section 2.2. Assume that there exists  $\{\tau_i\}_{i=1}^{d_y} \subset [1 : n]$  such that  $\bar{\alpha}_{\tau_i} \sigma_y^2 = (1 - \bar{\alpha}_{\tau_i}) s_i^2$ . Define for all  $i \in [1 : d_y]$ ,  $\tilde{\mathbf{y}}_i := \bar{\alpha}_{\tau_i}^{1/2} \mathbf{y}[i]$ . Then we can write the potential  $g_0^{\mathbf{y}}$  as the product of forward processes from time 0 to each time step  $\tau_i$ , i.e.

$$g_0^{\mathbf{y}}(\mathbf{x}_0) = \prod_{i=1}^{d_y} \bar{\alpha}_{\tau_i}^{1/2} \mathcal{N}(\tilde{\mathbf{y}}_i; \bar{\alpha}_{\tau_i}^{1/2} \mathbf{x}_0[i], (1 - \bar{\alpha}_{\tau_i})).$$

Writing the potential this way allows us to generalize (2.14) as follows. Denote for  $\ell \in [1 : d_x]$ ,  $\mathbf{x}^{\setminus \ell} \in \mathbb{R}^{d_x - 1}$  the vector  $\mathbf{x}$  with its  $\ell$ -th coordinate removed. Define

$$\phi_{\tau_1:n}^{\tilde{\mathbf{y}}} (d\mathbf{x}_{\tau_1:n}) \propto \left\{ \prod_{i=1}^{d_y-1} \lambda_{\tau_i|\tau_{i+1}}(\mathbf{x}_{\tau_i}|\mathbf{x}_{\tau_{i+1}}) \delta_{\tilde{\mathbf{y}}_i}(d\mathbf{x}_{\tau_i}[i]) d\mathbf{x}_{\tau_i}^{\setminus i} \right\} \mathfrak{p}_{\tau_{d_y}}(\mathbf{x}_{\tau_{d_y}}) \delta_{\tilde{\mathbf{y}}_{d_y}}(d\mathbf{x}_{\tau_{d_y}}[d_y]) d\mathbf{x}_{\tau_{d_y}}^{\setminus d_y},$$

which corresponds to the posterior of a noiseless inverse problem on the joint states  $\mathbf{X}_{\tau_1:n} \sim \mathfrak{p}_{\tau_1:n}$  with noiseless observations  $\tilde{\mathbf{y}}_{\tau_i}$  of  $\mathbf{X}_{\tau_i}[i]$  for all  $i \in [1 : d_y]$ .

**Proposition 2.3.** *Assume that  $\mathfrak{p}_{s+1}(\mathbf{x}_{s+1})\lambda_s(\mathbf{x}_s|\mathbf{x}_{s+1}) = \mathfrak{p}_s(\mathbf{x}_s)q_{s+1}(\mathbf{x}_{s+1}|\mathbf{x}_s)$  for all  $s \in [0 : n - 1]$ . Then it holds that*

$$\phi_0^{\mathbf{y}}(\mathbf{x}_0) \propto \int \lambda_{0|\tau_1}(\mathbf{x}_0|\mathbf{x}_{\tau_1}) \phi_{\tau_1:n}^{\tilde{\mathbf{y}}} (d\mathbf{x}_{\tau_1:n}).$$

The proof of Proposition 2.3 can be found in Appendix B.2. We have thus shown that sampling from the posterior  $\phi_0^{\mathbf{y}}$  is equivalent to sampling from the posterior  $\phi_{\tau_1:n}^{\tilde{\mathbf{y}}}$  then propagating the final state  $\mathbf{X}_{\tau_1}$  up to time 0 according to the backward kernel  $\lambda_{0|\tau_1}$ . Furthermore, we can extend the approximate recursion (2.15). For all  $t \in [\tau_1 : n]$  define  $\rho_t^{\tilde{\mathbf{y}}}(d\mathbf{x}_t) := \int \phi_{\tau_1:n}^{\tilde{\mathbf{y}}} (d\mathbf{x}_{\tau_1:n})$ , and for all  $s \in [0 : n - 1]$ ,  $z_s \in \mathbb{R}$  and  $\ell \in [1 : d_y]$ , let  $\lambda_s^{\ell}(z_s|\mathbf{x}_{s+1}) := \mathcal{N}(z_s; \mathfrak{m}_{s+1}(\mathbf{x}_{s+1})[\ell], \sigma_{s+1}^2)$ . By adapting the derivations of the previous section and using Lemma B.4, we find that the following approximate recursion is satisfied; for all  $k \in [1 : d_y]$  and  $t \in [\tau_k + 1, \tau_{k+1} - 1]$ ,

$$\rho_t^{\tilde{\mathbf{y}}}(\mathbf{x}_t) \approx \int \underline{\lambda}_t(\underline{\mathbf{x}}_t|\mathbf{x}_{t+1}) \prod_{\ell=\tau(t)+1}^{d_y} \lambda_t^{\ell}(\mathbf{x}_t[\ell]|\mathbf{x}_{t+1}) \prod_{j=1}^{\tau(t)} q_{t|\tau_j}^j(\mathbf{x}_t[j]|\tilde{\mathbf{y}}_j) \rho_{t+1}^{\tilde{\mathbf{y}}}(d\mathbf{x}_{t+1}), \quad (2.17)$$

where for all  $t \in [\tau_1 : n]$ ,  $\tau(t) := \max\{k \in [1 : d_y] : \tau_k \leq t\}$  and for all  $j \in [1 : d_y]$ , and  $t, s \in [1 : n]$  such that  $t > s$ ,  $q_{t|s}^j$  denotes the density of the  $j$ -th coordinate of the forward process from  $s$  to  $t$ . If  $t = \tau_k$ , then

$$\rho_t^{\tilde{\mathbf{y}}}(d\mathbf{x}_t) \approx \int \underline{\lambda}_t(d\mathbf{x}_t|\mathbf{x}_{t+1}) \delta_{\tilde{\mathbf{y}}_k}(d\mathbf{x}_t[k]) \prod_{\ell=\tau(t)+1}^{d_y} \lambda_t^{\ell}(d\mathbf{x}_t[\ell]|\mathbf{x}_{t+1}) \prod_{j=1}^{\tau(t)-1} q_{t|\tau_j}^j(d\mathbf{x}_t[j]|\tilde{\mathbf{y}}_j) \rho_{t+1}^{\tilde{\mathbf{y}}}(d\mathbf{x}_{t+1}).$$

We target the posterior  $\phi_0^{\mathbf{y}}$  by mimicking this recursion. Consider then  $\{g_t^y\}_{t=\tau}^n$  and sequence of probability measures  $\{\phi_t^{\mathbf{y}}\}_{t=\tau}^n$  defined for all  $t \in [\tau_1 : n]$  by  $\phi_t^{\mathbf{y}}(\mathbf{x}_t) \propto g_t^y(\mathbf{x}_t) \mathfrak{p}_t(\mathbf{x}_t)$  and

$$g_t^y : \mathbf{x}_t \mapsto \prod_{i=1}^{\tau(t)} \mathcal{N}(\mathbf{x}_t; \tilde{\mathbf{y}}_i, 1 - (1 - \kappa)\bar{\alpha}_t/\bar{\alpha}_{\tau_i}), \quad \kappa > 0. \quad (2.18)$$

We obtain a particle approximation of  $\phi_{\tau_1}^{\mathbf{y}}$  using a particle filter with proposal kernel and weight function

$$\lambda_t^{\mathbf{y}}(\mathbf{x}_t|\mathbf{x}_{t+1}) \propto g_t^y(\mathbf{x}_t) p_t(\mathbf{x}_t|\mathbf{x}_{t+1}), \quad \tilde{\omega}_t(\mathbf{x}_{t+1}) = \frac{\int g_t^y(\mathbf{x}_t) p_t(d\mathbf{x}_t|\mathbf{x}_{t+1})}{g_{t+1}^y(\mathbf{x}_{t+1})},$$

which are both available in closed form. Indeed, using standard Gaussian conjugation formulas, we find that

$$\lambda_t^{\mathbf{y}}(\mathbf{x}_t|\mathbf{x}_{t+1}) = \underline{\lambda}_t(\underline{\mathbf{x}}_t|\mathbf{x}_{t+1}) \prod_{k=\tau(t)+1}^{d_y} \lambda_t^k(\mathbf{x}_t[k]|\mathbf{x}_{t+1}) \prod_{\ell=1}^{\tau(t)} \lambda_t^{\mathbf{y},\ell}(\mathbf{x}_t[\ell]|\mathbf{x}_{t+1}), \quad (2.19)$$

where, by letting  $\sigma_{t|\tau_\ell}^2 := 1 - (1 - \kappa)\bar{\alpha}_t/\bar{\alpha}_{\tau_\ell}$  and  $\mathsf{K}_{t|\tau_\ell} = \sigma_{t+1}^2 / (\sigma_{t+1}^2 + \sigma_{t|\tau_\ell}^2)$ ,

$$\lambda_t^{\mathbf{y},\ell}(\mathbf{x}_t[\ell]|\mathbf{x}_{t+1}) = \mathcal{N}(\mathbf{x}_t[\ell]; \mathsf{K}_{t|\tau_\ell} \tilde{\mathbf{y}}_\ell + (1 - \mathsf{K}_{t|\tau_\ell}) \mathfrak{m}_{t+1}(\mathbf{x}_{t+1})[\ell], \mathsf{K}_{t|\tau_\ell} \sigma_{t|\tau_\ell}^2), \quad (2.20)$$

and

$$\tilde{\omega}_t(\mathbf{x}_{t+1}) = \prod_{\ell=1}^{\tau(t)} \frac{\mathcal{N}(\tilde{\mathbf{y}}_\ell; \mathbf{m}_{t+1}(\mathbf{x}_{t+1})[\ell], \sigma_{t+1}^2 + \sigma_{t|\tau_\ell}^2)}{\mathcal{N}(\mathbf{x}_{t+1}[\ell]; \tilde{\mathbf{y}}_\ell, \sigma_{t|\tau_\ell}^2)}. \quad (2.21)$$

Thus, applying Algorithm 1 with the transition kernels  $\{\lambda_t\}_{t=\tau_1}^{n-1}$  and weight function  $\{\tilde{\omega}_t\}_{t=\tau_1}^{n-1}$  yields the particle approximation  $\phi_{\tau_1}^N = N^{-1} \sum_{i=1}^N \delta_{\xi_{\tau_1}^i}$  and that of  $\phi_0^y$  is given by

$$\phi_0^N = \sum_{i=1}^N \omega_0^i \delta_{\xi_0^i}, \quad \text{where} \quad \xi_0^i \sim \lambda_{0|\tau}(\cdot | \xi_{\tau_1}^i), \quad \omega_0^i = \frac{g_0^y(\xi_0^i)/g_{\tau_1}^y(\xi_{\tau_1}^i)}{\sum_{j=1}^N g_0^y(\xi_0^j)/g_{\tau_1}^y(\xi_{\tau_1}^j)}.$$

### 3. NUMERICS

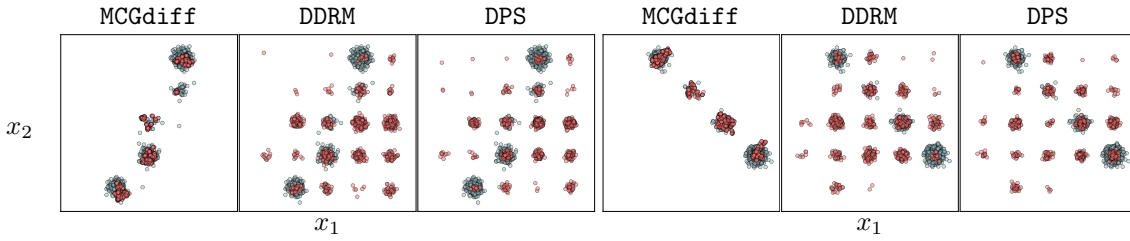


FIGURE 1. We display the first two dimensions of the GMM inverse problem for one of the measurement models tested. The blue dots represent samples from the exact posterior, while the red dots correspond to samples generated by each of the algorithms used (the names of the algorithms are given at the top of each column). The first three columns correspond to  $(d_x, d_y) = (80, 1)$  and the last three to  $(d_x, d_y) = (800, 1)$ . 20 steps of DDIM were used.

$d$	$d_y$	MCGdiff	DDRM	DPS	$d$	$d_y$	MCGdiff	DDRM	DPS
8	1	<b>2.6 ± 0.8</b>	6.9 ± 3.4	6.7 ± 1.1	8	1	<b>1.8 ± 0.6</b>	4.5 ± 1.5	3.3 ± 0.8
8	2	<b>1.0 ± 0.4</b>	4.6 ± 0.9	5.4 ± 1.3	8	2	<b>1.1 ± 0.5</b>	4.5 ± 1.3	3.2 ± 1.1
8	4	<b>0.5 ± 0.2</b>	1.8 ± 0.8	4.3 ± 1.1	8	4	<b>0.2 ± 0.0</b>	1.2 ± 0.6	0.9 ± 0.5
80	1	<b>2.2 ± 0.6</b>	7.7 ± 1.1	6.1 ± 1.2	80	1	<b>1.3 ± 0.3</b>	6.4 ± 1.2	3.1 ± 1.4
80	2	<b>0.9 ± 0.4</b>	9.9 ± 1.3	7.4 ± 1.4	80	2	<b>1.1 ± 0.7</b>	9.2 ± 1.1	2.8 ± 1.2
80	4	<b>0.4 ± 0.1</b>	7.8 ± 1.1	4.4 ± 1.1	80	4	<b>0.3 ± 0.0</b>	7.1 ± 1.0	1.4 ± 0.6
800	1	<b>2.3 ± 0.8</b>	7.7 ± 0.8	6.5 ± 0.8	800	1	<b>2.6 ± 0.9</b>	7.2 ± 1.4	2.7 ± 1.0
800	2	<b>1.8 ± 0.8</b>	8.6 ± 0.8	6.5 ± 1.1	800	2	<b>1.3 ± 0.8</b>	8.6 ± 1.0	1.8 ± 0.9
800	4	<b>0.7 ± 0.5</b>	9.5 ± 0.9	5.5 ± 0.9	800	4	<b>0.3 ± 0.0</b>	8.3 ± 1.0	0.4 ± 0.2

TABLE 1. Sliced Wasserstein for the GMM case. Table on the left correspond to 20 steps of DDIM with  $\eta = 0.6$  and on the right to 100 steps and  $\eta = 0.85$ .

**Gaussian Mixture Model.** We present an example where the data distribution  $\mathbf{q}_{\text{data}}$  is a mixture of 25 Gaussian distributions. The means and variances of the components of the mixture are given in Appendix B.3. In this case, for each choice of forward operator  $\mathbf{A}$  and measurement noise standard deviation  $\sigma_y > 0$ , the target posterior distribution  $\phi_0^y$  can be computed explicitly, see Appendix B.3. Moreover, it is possible to explicitly minimize each term occurring in the denoising problem (1.9), so that the choice of the weighting scheme  $\{\sigma_t\}_{t \in \mathbb{N}}$  is irrelevant. To investigate the performance of posterior sampling methods, for each pair of dimensions  $(d_x, d_y) \in \{8, 80, 800\} \times \{1, 2, 4\}$  we randomly generate multiple measurement models  $(y, \mathbf{A}, \sigma_y) \in \mathbb{R}^{d_y} \times \mathbb{R}^{d_y \times d_x} \times [0, 1]$ , and we also randomly choose the weight



FIGURE 2. Inpainting with different masks on the CelebA test set.

associated with each component of the Gaussian mixture. Details (distribution of  $A$ ,  $\sigma_y$ , etc...) are given in Appendix B.3. This example is particularly interesting because it allows us to study the behaviour of our method on difficult and ill-posed problems in high dimensions while having access to the exact posterior with which to compare – obtaining a "ground truth" for the posterior is not feasible for most problems. By varying the dimension, the forward operator, the noise level, and the mixture weight, we gain insight into the performance of posterior sampling methods under varying conditions and with different levels of posterior multimodality.

To compare the posterior distribution estimated by each algorithm with the exact target posterior distribution, we use the sliced Wasserstein (SW) distance defined in Appendix B.3. We use  $10^4$  slices for the SW distance and compare 1000 samples of MCGdiff, DPS, and DDRM with 1000 samples of the true posterior distribution obtained using 20 DDIM steps and 100 DDIM steps for generation. The variance reduction DDIM parameter  $\eta$  is set to 0.6 and 0.85 for the 20 and 100 DDIM steps, respectively. When choosing the timesteps of DDIM we want to emulate the constraint  $\sigma_y^2 \alpha_{\tau_i} = (1 - \alpha_{\tau_i}) s_i^2$ . Therefore, we include the timesteps  $t$  that minimizes  $|\sigma_y^2 \alpha_t - (1 - \alpha_t) s_i^2|$  for each  $i \in [1 : d_y]$ . More details are given in Appendix B.3.

Table 1 indicates the CLT 95% confidence intervals obtained by considering 20 randomly selected measurement models  $(y, A, \sigma_y)$  for each setting  $(d_x, d_y)$ . Figure 1 shows the first two dimensions of the estimated posterior distributions corresponding to the configurations  $(80, 1)$  and  $(800, 1)$  from Table 1 for one of the randomly generated measurement model  $(y, A, \sigma_y)$  in the case of 20 DDIM steps. Illustration of other settings are given in Appendix B.3. These illustrations give us insight into the behaviour of the algorithms and their ability to accurately estimate the posterior distribution. We see that MCGdiff is more precise at estimating the posterior distribution and does not sample outside of the support of the posterior distribution in all scenarios tested. Table 1 also shows that the difference in performance is greater in the more extreme settings where the problem is ill-posed ( $d_y = 1, 2$ ) and the number of DDIM steps is limited (20).

**Inpainting.** We consider the inpainting problem on the CelebA dataset. The images dimension are  $3 \times 256 \times 256$  and we use pretrained denoising network available at <https://github.com/bahjat-kawar/ddrm> for all the methods. All methods share the same DDIM parameters, with 250 sample steps between  $[0 : 1000]$  and  $\eta = 1$ . For MCGdiff and SMCdiff, a total of  $N = 384$  particles is used. For DPS we set the learning rate parameter to  $\zeta_i = 0.5$  and for DDRM we consider the configuration proposed on

[Kawar et al., ]. We also use several different masks on images from the CelebA test set in fig. 2. The first row corresponds to samples from the most ill-posed problem.

Next, we compare **MCGdiff** to **DPS** and **DDRM** on several different noisy inverse problems over several different image datasets (section 3). For each algorithm, we generate 1000 samples and we show the pair of samples that are the furthest apart in  $L^2$  norm from each other in the pool of samples. For **MCGdiff** we ran several parallel particle filters with  $N = 64$  to generate 1000 samples.

	CIFAR-10	Flowers	Cats	Bedroom	Church	CelebaHQ
$(W, H, C)$	$(32, 32, 3)$	$(64, 64, 3)$	$(128, 128, 3)$	$(256, 256, 3)$	$(256, 256, 3)$	$(256, 256, 3)$

TABLE 2. The datasets used for the inverse problems over image datasets.

**Super Resolution.** We compare for the super resolution problem. We set  $\sigma_y = 0.05$  for all the datasets and  $\zeta_{\text{coeff}} = 0.1$  for **DPS**. We use 100 steps of **DDIM** with  $\eta = 1$ . The results are shown in Figure 3. We use a downsampling ratio of 4 for the CIFAR-10 dataset, 8 for both Flowers and Cats datasets and 16 for the others.

**Gaussian 2D deblurring.** We consider a Gaussian 2D square kernel with sizes  $(w/6, h/6)$  and standard deviation  $w/30$  where  $(w, h)$  are the width and height of the image. We set  $\sigma_y = 0.1$  for all the datasets and  $\zeta_{\text{coeff}} = 0.1$  for **DPS**. We use 100 steps of **DDIM** with  $\eta = 1$ . The results are shown in Figure 4.

#### 4. CONCLUSION

In this paper, we have introduced **MCGdiff** a novel method for solving Bayesian linear Gaussian inverse problems with a denoising diffusion based generative model prior. We have shown that **MCGdiff** is theoretically grounded and provided numerical experiments that reflect the adequacy of **MCGdiff** in a Bayesian framework, as opposed to recent works. This difference is of the utmost importance when the relevance of the generated samples is hard to verify, as in safety critical applications. **MCGdiff** is a first step towards robust approaches for addressing the challenges of Bayesian linear inverse problems with denoising diffusion based generative model priors.

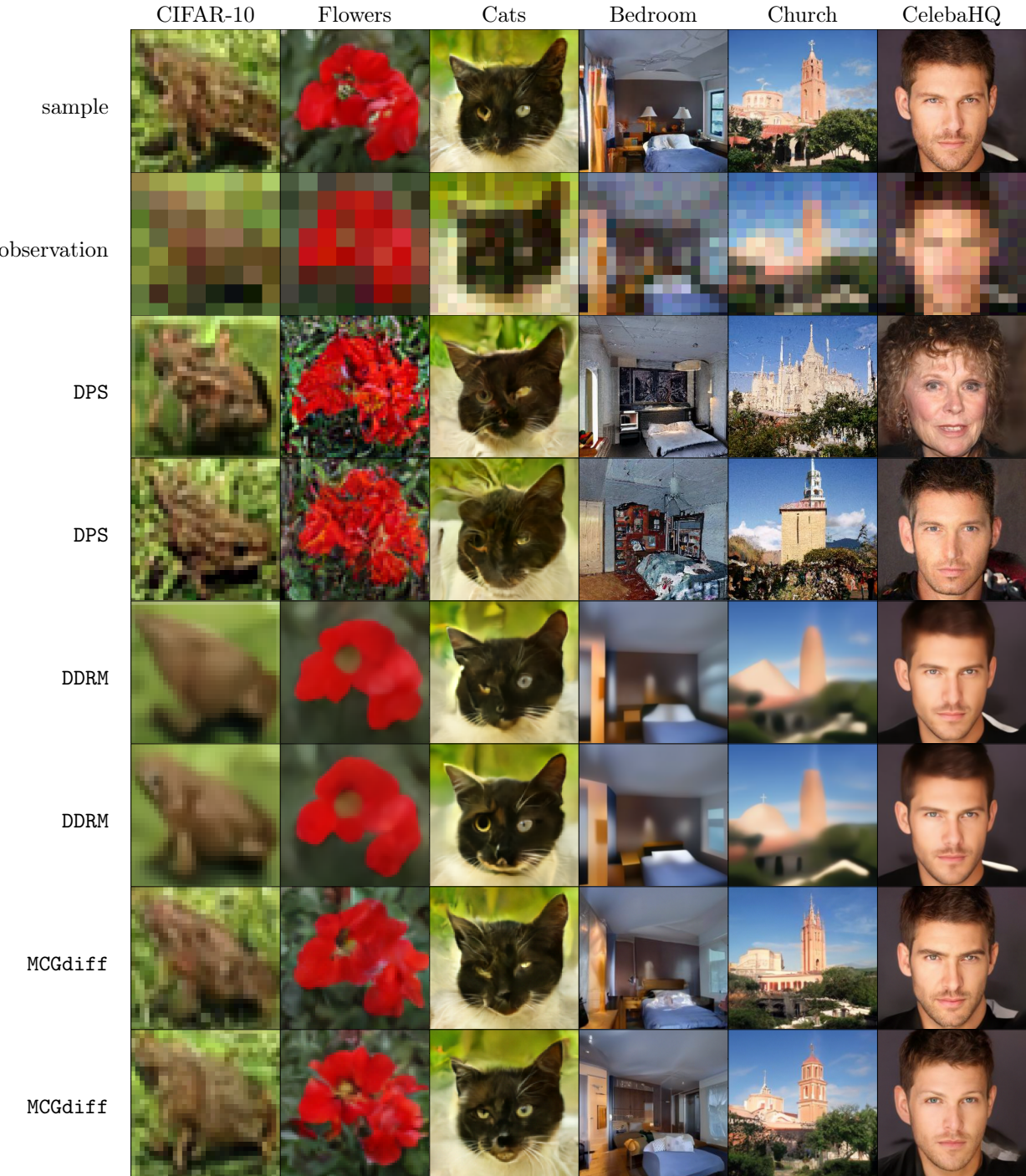


FIGURE 3. Ratio 4 for CIFAR, 8 for flowers and Cats and 16 for CELEB

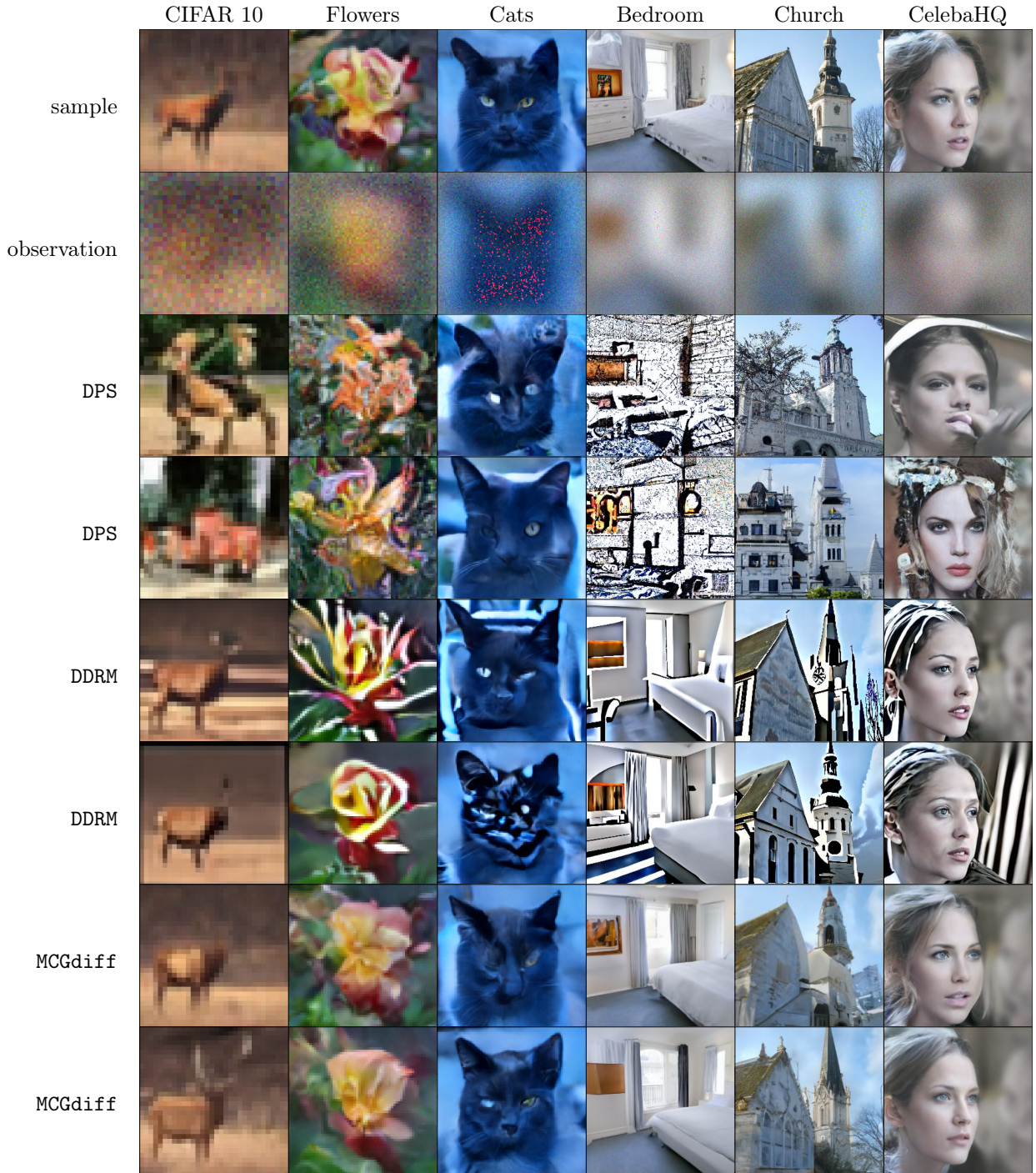


FIGURE 4

## REFERENCES

[Andrieu et al., 2018] Andrieu, C., Lee, A., and Vihola, M. (2018). Uniform ergodicity of the iterated conditional SMC and geometric ergodicity of particle Gibbs samplers. *Bernoulli*, 24(2):842 – 872.

[Arjomand Bigdeli et al., 2017] Arjomand Bigdeli, S., Zwicker, M., Favaro, P., and Jin, M. (2017). Deep mean-shift priors for image restoration. *Advances in Neural Information Processing Systems*, 30.

[Benton et al., 2022] Benton, J., Shi, Y., De Bortoli, V., Deligiannidis, G., and Doucet, A. (2022). From denoising diffusions to denoising markov models. *arXiv preprint arXiv:2211.03595*.

[Besag et al., 1991] Besag, J., York, J., and Mollié, A. (1991). Bayesian image restoration, with two applications in spatial statistics. *Annals of the institute of statistical mathematics*, 43:1–20.

[Cappé et al., 2005] Cappé, O., Moulines, E., and Ryden, T. (2005). *Inference in Hidden Markov Models (Springer Series in Statistics)*. Springer-Verlag, Berlin, Heidelberg.

[Cheney and Borden, 2009] Cheney, M. and Borden, B. (2009). *Fundamentals of radar imaging*. SIAM.

[Chopin et al., 2020] Chopin, N., Papaspiliopoulos, O., et al. (2020). *An introduction to sequential Monte Carlo*, volume 4. Springer.

[Chung et al., 2023] Chung, H., Kim, J., Mccann, M. T., Klasky, M. L., and Ye, J. C. (2023). Diffusion posterior sampling for general noisy inverse problems. In *The Eleventh International Conference on Learning Representations*.

[Dashti and Stuart, 2017] Dashti, M. and Stuart, A. M. (2017). The bayesian approach to inverse problems. In *Handbook of uncertainty quantification*, pages 311–428. Springer.

[Douc et al., 2014] Douc, R., Moulines, E., and Stoffer, D. (2014). *Nonlinear time series: Theory, methods and applications with R examples*. CRC press.

[Doucet et al., 2001] Doucet, A., De Freitas, N., Gordon, N. J., et al. (2001). *Sequential Monte Carlo methods in practice*, volume 1. Springer.

[Elbakri and Fessler, 2002] Elbakri, I. A. and Fessler, J. A. (2002). Statistical image reconstruction for polyenergetic x-ray computed tomography. *IEEE transactions on medical imaging*, 21(2):89–99.

[Fergus et al., 2006] Fergus, R., Singh, B., Hertzmann, A., Roweis, S. T., and Freeman, W. T. (2006). Removing camera shake from a single photograph. In *AcM Siggraph 2006 Papers*, pages 787–794.

[Figueiredo et al., 2007] Figueiredo, M. A., Bioucas-Dias, J. M., and Nowak, R. D. (2007). Majorization–minimization algorithms for wavelet-based image restoration. *IEEE Transactions on Image processing*, 16(12):2980–2991.

[González et al., 2009] González, R. C., Woods, R. E., and Masters, B. R. (2009). *Digital image processing*, third edition. *Journal of Biomedical Optics*, 14:029901.

[Gui et al., 2021] Gui, J., Sun, Z., Wen, Y., Tao, D., and Ye, J. (2021). A review on generative adversarial networks: Algorithms, theory, and applications. *IEEE transactions on knowledge and data engineering*.

[Ho et al., 2020] Ho, J., Jain, A., and Abbeel, P. (2020). Denoising diffusion probabilistic models. *Advances in Neural Information Processing Systems*, 33:6840–6851.

[Huggins and Roy, 2019] Huggins, J. H. and Roy, D. M. (2019). Sequential Monte Carlo as approximate sampling: bounds, adaptive resampling via  $\infty$ -ESS, and an application to particle Gibbs. *Bernoulli*, 25(1):584 – 622.

[Idier, 2013] Idier, J. (2013). *Bayesian approach to inverse problems*. John Wiley & Sons.

[Ivanov et al., 2018] Ivanov, O., Figurnov, M., and Vetrov, D. (2018). Variational autoencoder with arbitrary conditioning. *arXiv preprint arXiv:1806.02382*.

[Kaipio et al., 2000] Kaipio, J. P., Kolehmainen, V., Somersalo, E., and Vauhkonen, M. (2000). Statistical inversion and monte carlo sampling methods in electrical impedance tomography. *Inverse problems*, 16(5):1487.

[Kaltenbach et al., 2023] Kaltenbach, S., Perdikaris, P., and Koutsourelakis, P.-S. (2023). Semi-supervised invertible neural operators for bayesian inverse problems. *Computational Mechanics*, pages 1–20.

[Kawar et al., ] Kawar, B., Elad, M., Ermon, S., and Song, J. Denoising diffusion restoration models. In *Advances in Neural Information Processing Systems*.

[Kingma et al., 2019] Kingma, D. P., Welling, M., et al. (2019). An introduction to variational autoencoders. *Foundations and Trends® in Machine Learning*, 12(4):307–392.

[Kobyzev et al., 2020] Kobyzev, I., Prince, S. J., and Brubaker, M. A. (2020). Normalizing flows: An introduction and review of current methods. *IEEE transactions on pattern analysis and machine intelligence*, 43(11):3964–3979.

[Lugmayr et al., 2022] Lugmayr, A., Danelljan, M., Romero, A., Yu, F., Timofte, R., and Van Gool, L. (2022). Repaint: Inpainting using denoising diffusion probabilistic models. In *Proceedings of the IEEE/CVF Conference on Computer Vision and Pattern Recognition*, pages 11461–11471.

[Marnissi et al., 2017] Marnissi, Y., Zheng, Y., Chouzenoux, E., and Pesquet, J.-C. (2017). A variational bayesian approach for image restoration—application to image deblurring with poisson–gaussian noise. *IEEE Transactions on Computational Imaging*, 3(4):722–737.

[Peng et al., 2021] Peng, J., Liu, D., Xu, S., and Li, H. (2021). Generating diverse structure for image inpainting with hierarchical vqv-vae. In *Proceedings of the IEEE/CVF Conference on Computer Vision and Pattern Recognition*, pages 10775–10784.

[Pitt and Shephard, 1999] Pitt, M. K. and Shephard, N. (1999). Filtering via simulation: Auxiliary particle filters. *Journal of the American statistical association*, 94(446):590–599.

[Sahlström and Tarvainen, 2023] Sahlström, T. and Tarvainen, T. (2023). Utilizing variational autoencoders in the bayesian inverse problem of photoacoustic tomography. *SIAM Journal on Imaging Sciences*, 16(1):89–110.

[Shin and Choi, 2023] Shin, H. and Choi, M. (2023). Physics-informed variational inference for uncertainty quantification of stochastic differential equations. *Journal of Computational Physics*, page 112183.

[Sohl-Dickstein et al., 2015] Sohl-Dickstein, J., Weiss, E., Maheswaranathan, N., and Ganguli, S. (2015). Deep unsupervised learning using nonequilibrium thermodynamics. In *International Conference on Machine Learning*, pages 2256–2265. PMLR.

[Song et al., 2021a] Song, J., Meng, C., and Ermon, S. (2021a). Denoising diffusion implicit models. In *International Conference on Learning Representations*.

[Song et al., 2021b] Song, Y., Durkan, C., Murray, I., and Ermon, S. (2021b). Maximum likelihood training of score-based diffusion models. *Advances in Neural Information Processing Systems*, 34:1415–1428.

[Song et al., 2022] Song, Y., Shen, L., Xing, L., and Ermon, S. (2022). Solving inverse problems in medical imaging with score-based generative models. In *International Conference on Learning Representations*.

[Song et al., 2021c] Song, Y., Sohl-Dickstein, J., Kingma, D. P., Kumar, A., Ermon, S., and Poole, B. (2021c). Score-based generative modeling through stochastic differential equations. In *International Conference on Learning Representations*.

[Stuart, 2010] Stuart, A. M. (2010). Inverse problems: a bayesian perspective. *Acta numerica*, 19:451–559.

[Su et al., 2022] Su, J., Xu, B., and Yin, H. (2022). A survey of deep learning approaches to image restoration. *Neurocomputing*, 487:46–65.

[Trippe et al., 2023] Trippe, B. L., Yim, J., Tischer, D., Baker, D., Broderick, T., Barzilay, R., and Jaakkola, T. S. (2023). Diffusion probabilistic modeling of protein backbones in 3d for the motif-scaffolding problem. In *The Eleventh International Conference on Learning Representations*.

[Vlaardingerbroek and Boer, 2013] Vlaardingerbroek, M. T. and Boer, J. A. (2013). *Magnetic resonance imaging: theory and practice*. Springer Science & Business Media.

[Wan et al., 2021] Wan, Z., Zhang, J., Chen, D., and Liao, J. (2021). High-fidelity pluralistic image completion with transformers. In *Proceedings of the IEEE/CVF International Conference on Computer Vision*, pages 4692–4701.

[Wei et al., 2022] Wei, X., van Gorp, H., Gonzalez-Carabarin, L., Freedman, D., Eldar, Y. C., and van Sloun, R. J. (2022). Deep unfolding with normalizing flow priors for inverse problems. *IEEE Transactions on Signal Processing*, 70:2962–2971.

[Xiang et al., 2023] Xiang, H., Zou, Q., Nawaz, M. A., Huang, X., Zhang, F., and Yu, H. (2023). Deep learning for image inpainting: A survey. *Pattern Recognition*, 134:109046.

[Yeh et al., 2018] Yeh, R. A., Lim, T. Y., Chen, C., Schwing, A. G., Hasegawa-Johnson, M., and Do, M. N. (2018). Image restoration with deep generative models. In *2018 IEEE International Conference on Acoustics, Speech and Signal Processing (ICASSP)*, pages 6772–6776. IEEE.

[Yu et al., 2018] Yu, J., Lin, Z., Yang, J., Shen, X., Lu, X., and Huang, T. S. (2018). Generative image inpainting with contextual attention. In *Proceedings of the IEEE conference on computer vision and pattern recognition*, pages 5505–5514.

[Zeng et al., 2022] Zeng, Y., Fu, J., Chao, H., and Guo, B. (2022). Aggregated contextual transformations for high-resolution image inpainting. *IEEE Transactions on Visualization and Computer Graphics*.

[Zhang et al., 2023] Zhang, G., Ji, J., Zhang, Y., Yu, M., Jaakkola, T., and Chang, S. (2023). Towards coherent image inpainting using denoising diffusion implicit models. *arXiv preprint arXiv:2304.03322*.

[Zheng et al., 2019] Zheng, C., Cham, T.-J., and Cai, J. (2019). Pluralistic image completion. In *Proceedings of the IEEE/CVF Conference on Computer Vision and Pattern Recognition*, pages 1438–1447.

[Zhihang et al., 2023] Zhihang, X., Yingzhi, X., and Qifeng, L. (2023). A domain-decomposed vae method for bayesian inverse problems. *arXiv preprint arXiv:2301.05708*.

## APPENDIX A. SMCdiff EXTENSION

The identity (2.14) allows us to extend **SMCdiff** [Trippe et al., 2023] to handle noisy inverse problems as we now show. We have that

$$\begin{aligned}\phi_{\tau}^{\tilde{y}_{\tau}}(\underline{x}_{\tau}) &= \frac{\int p_{\tau}(\tilde{y}_{\tau} \cap \underline{x}_{\tau} | x_{\tau+1}) \left\{ \prod_{s=\tau+1}^{n-1} p_s(dx_s | x_{s+1}) \right\} \mathbf{p}_n(dx_n)}{\int \mathbf{p}_{\tau}(\tilde{y}_{\tau} \cap \underline{z}_{\tau}) d\underline{z}_{\tau}} \\ &= \int b_{\tau:n}^{\tilde{y}_{\tau}}(\underline{x}_{\tau:n} | \bar{x}_{\tau+1:n}) f_{\tau+1:n}^{\tilde{y}_{\tau}}(d\bar{x}_{\tau+1:n}) d\underline{x}_{\tau+1:n},\end{aligned}$$

where

$$\begin{aligned}b_{\tau:n}(\underline{x}_{\tau:n} | \bar{x}_{\tau+1:n}) &= \frac{p_{\tau}(\tilde{y}_{\tau} \cap \underline{x}_{\tau} | x_{\tau+1}) \left\{ \prod_{s=\tau+1}^{n-1} \underline{p}_s(x_s | x_{s+1}) \bar{p}_s(\bar{x}_s | x_{s+1}) \right\} \underline{\mathbf{p}}_n(\underline{x}_n)}{\mathsf{L}_{\tau:n}^{\tilde{y}_{\tau}}(\bar{x}_{\tau+1:n})}, \\ f_{\tau+1:n}^{\tilde{y}_{\tau}}(\bar{x}_{\tau+1:n}) &= \frac{\mathsf{L}_{\tau:n}^{\tilde{y}_{\tau}}(\bar{x}_{\tau+1:n})}{\int \mathbf{p}_{\tau}(\tilde{y}_{\tau} \cap \underline{z}_{\tau}) d\underline{z}_{\tau}},\end{aligned}$$

and

$$\mathsf{L}_{\tau:n}^{\tilde{y}_{\tau}}(\bar{x}_{\tau+1:n}) = \int p_{\tau}(\tilde{y}_{\tau} \cap \underline{z}_{\tau} | \bar{x}_{\tau+1} \cap \underline{z}_{\tau+1}) \left\{ \prod_{s=\tau+1}^{n-1} \underline{p}_s(d\underline{z}_s | \bar{x}_{s+1} \cap \underline{z}_{s+1}) \bar{p}_s(\bar{x}_s | \bar{x}_{s+1} \cap \underline{z}_{s+1}) \right\} \underline{\mathbf{p}}_n(d\underline{z}_n).$$

Next, (2.13) implies that

$$\begin{aligned}\int \mathbf{p}_{s+1}(\bar{x}_{s+1} \cap \underline{z}_{s+1}) \underline{p}_s(d\underline{z}_s | \bar{x}_{s+1} \cap \underline{z}_{s+1}) \bar{p}_s(\bar{x}_s | \bar{x}_{s+1} \cap \underline{z}_{s+1}) d\underline{z}_{s:s+1} = \\ \int \mathbf{p}_s(\bar{x}_s \cap \underline{z}_s) \bar{q}_{s+1}(\bar{x}_{s+1} | \bar{x}_s) q_{s+1}(\underline{z}_{s+1} | \underline{z}_s) d\underline{z}_{s:s+1},\end{aligned}$$

and applied repeatedly, we find that

$$\mathsf{L}_{\tau}^{\tilde{y}_{\tau}}(\bar{x}_{\tau+1:n}) = \int \mathbf{p}_{\tau}(\tilde{y}_{\tau} \cap \underline{x}_{\tau}) d\underline{x}_{\tau} \cdot \int \delta_{\tilde{y}_{\tau}}(d\bar{x}_{\tau}) \prod_{s=\tau+1}^n \bar{q}_s(\bar{x}_s | \bar{x}_{s-1}).$$

and thus,  $f_{\tau:n}^{\tilde{y}_{\tau}}(\bar{x}_{\tau+1:n}) = \int \delta_{\tilde{y}_{\tau}}(d\bar{x}_{\tau}) \prod_{s=\tau+1}^n \bar{q}_s(\bar{x}_s | \bar{x}_{s-1})$ . In order to approximate  $\phi_{\tau}^{\tilde{y}_{\tau}}$  we first diffuse the noised observation up to time  $n$ , resulting in  $\bar{x}_{\tau+1:n}$ , and then estimate  $b_{\tau+1:n}^{\tilde{y}_{\tau}}(\cdot | \bar{x}_{\tau+1:n})$  using a particle filter with  $\underline{p}_s(\underline{x}_s | x_{s+1})$  as transition kernel at step  $s \in [\tau+1 : n]$  and  $g_s : \underline{z}_s \mapsto \bar{p}_{s-1}(\bar{x}_{s-1} | \bar{x}_s \cap \underline{z}_s)$  as potential, similarly to **SMCdiff**.

## APPENDIX B. PROOFS

## B.1. Proof of Proposition 2.2.

**Preliminary definitions.** We preface the proof with notations and definitions of a few quantities that will be used throughout.

For a probability measure  $\mu$  and  $f$  a bounded measurable function, we write  $\mu(f) := \int f(x)\mu(dx)$  the expectation of  $f$  under  $\mu$  and if  $K(dx|z)$  is a transition kernel we write  $K(f)(z) := \int f(x)K(dx|z)$ .

Define the *smoothing* distribution

$$\phi_{0:n}^y(dx_{0:n}) \propto \delta_y(d\bar{x}_0) \mathbf{p}_{0:n}(x_{0:n}) d\underline{x}_0 dx_{1:n}, \quad (\text{B.1})$$

which admits the posterior  $\phi_0^y$  as time 0 marginal. Its particle estimate known as the *poor man smoother* is given by

$$\phi_{0:n}^N(dx_{0:n}) = N^{-1} \sum_{k_{0:n} \in [1:N]^{n+1}} \delta_{y \cap \underline{\xi}_0^{k_0}}(dx_0) \prod_{s=1}^n \mathbb{1}\{k_s = I_s^{k_{s-1}}\} \delta_{\xi_s^{k_s}}(dx_s). \quad (\text{B.2})$$

We also let  $\Phi_{0:n}^N$  be the probability measure defined for any  $B \in \mathcal{B}(\mathbb{R}^{\mathbf{d}_x})^{\otimes n+1}$  by

$$\Phi_{0:n}^N(B) = \mathbb{E}[\phi_{0:n}^N(B)],$$

where the expectation is with respect to the probability measure

$$\begin{aligned} P_{0:n}^N(d(x_{0:n}^{1:N}, a_{1:n}^{1:N})) &= \prod_{i=1}^N p_n^y(dx_n^i) \prod_{\ell=2}^n \left\{ \prod_{j=1}^N \sum_{k=1}^N \omega_{\ell-1}^k \delta_k(da_\ell^j) p_{\ell-1}^y(dx_{\ell-1}^j | x_\ell^{a_\ell^j}) \right\} \\ &\quad \times \prod_{j=1}^N \sum_{k=1}^N \omega_0^k \delta_k(da_1^j) p_0^y(dx_0^j | x_1^{a_1^j}) \delta_y(d\bar{x}_0^j), \end{aligned} \quad (\text{B.3})$$

where  $\omega_t^i := \tilde{\omega}_t(\xi_{t+1}^i) / \sum_{j=1}^N \tilde{\omega}_t(\xi_{t+1}^j)$  and which corresponds to the joint law of all the random variables generated by Algorithm 1. It then follows by definition that for any  $C \in \mathcal{B}(\mathbb{R}^{\mathbf{d}_x})$ ,

$$\int \Phi_{0:n}^N(dz_{0:n}) \mathbb{1}_C(z_0) = \mathbb{E} \left[ \int \phi_{0:n}^N(dz_{0:n}) \mathbb{1}_C(z_0) \right] = \mathbb{E}[\phi_0^N(C)] = \Phi_0^N(C).$$

Define also the law of the *conditional* particle cloud

$$\begin{aligned} \mathbf{P}^N(d(x_{0:n}^{1:N}, a_{1:n}^{1:N}) | z_{0:n}) &= \delta_{z_n}(dx_n^N) \prod_{i=1}^{N-1} p_n^y(dx_n^i) \\ &\quad \times \prod_{\ell=2}^n \delta_{z_{\ell-1}}(dx_{\ell-1}^N) \delta_N(da_{\ell-1}^N) \prod_{j=1}^{N-1} \sum_{k=1}^N \omega_{\ell-1}^k \delta_k(da_\ell^j) p_{\ell-1}^y(dx_{\ell-1}^j | x_\ell^{a_\ell^j}) \\ &\quad \times \delta_{z_0}(dx_0^N) \delta_N(da_1^N) \prod_{j=1}^{N-1} \sum_{k=1}^N \omega_0^k \delta_k(da_1^j) p_0^y(dx_0^j | x_1^{a_1^j}) \delta_y(d\bar{x}_0^j). \end{aligned} \quad (\text{B.4})$$

In what follows  $\mathbb{E}_{z_{0:n}}$  refers to expectation with respect to  $\mathbf{P}^N(\cdot | z_{0:n})$ . Finally, for  $s \in [0 : n-1]$  we let  $\Omega_s^N$  denote the sum of the filtering weights at step  $s$ , i.e.  $\Omega_s^N = \sum_{i=1}^N \tilde{\omega}_s(\xi_{s+1}^i)$ . We also write  $\mathcal{Z}_0 = \int p_0(x_0) \delta_y(d\bar{x}_0) dx_0$  and for all  $\ell \in [1 : n]$ ,  $\mathcal{Z}_\ell = \int \bar{q}_{\ell|0}(\bar{x}_\ell | y) p_\ell(dx_\ell)$ .

The proof of Proposition 2.2 relies on two Lemmata stated below and proved in Appendix B.1; in Lemma B.1 we provide an expression for the Radon-Nikodym derivative  $d\phi_{0:n}^y/d\Phi_{0:n}^y$  and in Lemma B.2 we explicit its leading term.

**Lemma B.1.**  $\phi_{0:n}^y$  and  $\Phi_{0:n}^N$  are equivalent and we have that

$$\Phi_{0:n}^N(dz_{0:n}) = \mathbb{E}_{z_{0:n}} \left[ \frac{N^n \mathcal{Z}_0 / \mathcal{Z}_0}{\prod_{s=0}^{n-1} \Omega_s^N} \right] \phi_{0:n}^y(dz_{0:n}). \quad (\text{B.5})$$

**Lemma B.2.** It holds that

$$\begin{aligned} \frac{\mathcal{Z}_n}{\mathcal{Z}_0} \mathbb{E}_{z_{0:n}} \left[ \prod_{s=0}^{n-1} N^{-1} \Omega_s^N \right] &= \left( \frac{N-1}{N} \right)^n \\ &\quad + \frac{(N-1)^{n-1}}{N^n} \sum_{s=1}^n \frac{\mathcal{Z}_s / \mathcal{Z}_0}{\bar{q}_{s|0}(\bar{z}_s | y)} \int p_{0|s}(x_0 | z_s) \delta_y(d\bar{x}_0) dx_0 + \frac{D_{0:n}^y}{N^2}. \end{aligned} \quad (\text{B.6})$$

where  $D_{0:n}^y$  is a positive constant.

Before proceeding with the proof of Proposition 2.2, let us note that having  $z \mapsto \tilde{\omega}_\ell(z)$  bounded on  $\mathbb{R}^{\mathbf{d}_x}$  for all  $\ell \in [0 : n-1]$  is sufficient to guarantee that  $C_{0:n}^y$  and  $D_{0:n}^y$  are finite since in this case it follows immediately that  $\mathbb{E}_{z_{0:n}} \left[ \prod_{s=0}^{n-1} N^{-1} \Omega_s^N \right]$  is bounded and so is the right hand side of (B.6). This can be

achieved with a slight modification of (2.5) and (2.6). Indeed, consider instead the following recursion for  $s \in [0 : n]$  where  $\delta > 0$ ,

$$\begin{aligned}\phi_n^y(x_n) &\propto (\bar{q}_{n|0}(\bar{x}_n|y) + \delta) \mathbf{p}_n(x_n), \\ \phi_s^y(x_s) &\propto \int \phi_{s+1}^y(x_{s+1}) p_s(dx_s|x_{s+1}) \frac{\bar{q}_s(\bar{x}_s|y) + \delta}{\bar{q}_{s+1}(\bar{x}_{s+1}|y) + \delta} dx_{s+1}.\end{aligned}$$

Then we have that

$$\phi_0^y(x_0) \propto \int \phi_1^y(x_1) \underline{p}_0(x_0|x_1) \frac{\bar{p}_0(y|x_1)}{\bar{q}_{1|0}(\bar{x}_1|y) + \delta} dx_1.$$

We can then use Algorithm 1 to produce a particle approximation of  $\phi_0^y$  using the following transition and weight function,

$$\begin{aligned}p_s^{y,\delta}(x_s|x_{s+1}) &= \frac{\gamma_s(y|x_{s+1})}{\gamma_s(y|x_{s+1}) + \delta} p_s^y(x_s|x_{s+1}) + \frac{\delta}{\gamma_s(y|x_{s+1}) + \delta} p_s(x_s|x_{s+1}), \\ \tilde{\omega}_s(x_{s+1}) &= (\gamma_s(y|x_{s+1}) + \delta) / (\bar{q}_{s+1|0}(\bar{x}_{s+1}|y) + \delta),\end{aligned}$$

where  $\gamma_s(y|x_{s+1}) = \int \bar{q}_{s|0}(\bar{x}_s|y) p_s(x_s|x_{s+1}) dx_s$  is available in closed form and  $p_s^y$  is defined in (2.3).  $\tilde{\omega}_s$  is thus clearly bounded for all  $s \in [0 : n - 1]$  and it is still possible to sample from  $p_s^{y,\delta}$  since it is simply a mixture between the transition (2.3) and the ‘‘prior’’ transition.

*Proof of Proposition 2.2.* Consider the *forward* Markov kernel

$$\vec{\mathbf{B}}_{1:n}(z_0, dz_{1:n}) = \frac{\mathbf{p}_{1:n}(dz_{1:n}) p_0(z_0|z_1)}{\int \mathbf{p}_{1:n}(d\tilde{z}_{1:n}) p_0(\tilde{z}_0|\tilde{z}_1)}, \quad (\text{B.7})$$

which satisfies

$$\phi_{0:n}^y(dz_{0:n}) = \phi_0^y(dz_0) \vec{\mathbf{B}}_{1:n}(z_0, dz_{1:n}).$$

By Lemma B.1 we have for any  $C \in \mathcal{B}(\mathbb{R}^{d_x})$  that

$$\begin{aligned}\Phi_0^N(C) &= \int \Phi_{0:n}^N(dz_{0:n}) \mathbb{1}_C(z_0) \\ &= \int \mathbb{1}_C(z_0) \mathbb{E}_{z_{0:n}} \left[ \frac{N^n \mathcal{Z}_0 / \mathcal{Z}_n}{\prod_{s=0}^{n-1} \Omega_s^N} \right] \phi_{0:n}^y(dz_{0:n}) \\ &= \int \mathbb{1}_C(z_0) \int \vec{\mathbf{B}}_{1:n}(z_0, dz_{1:n}) \mathbb{E}_{z_{0:n}} \left[ \frac{N^n \mathcal{Z}_0 / \mathcal{Z}_n}{\prod_{s=0}^{n-1} \Omega_s^N} \right] \phi_0^y(dz_0),\end{aligned}$$

which shows that the Radon-Nikodym derivative  $d\Phi_0^N/d\phi_0^y$  is,

$$\frac{d\Phi_0^N}{d\phi_0^y}(z_0) = \int \vec{\mathbf{B}}_{1:n}(z_0, dz_{1:n}) \mathbb{E}_{z_{0:n}} \left[ \frac{N^n \mathcal{Z}_0 / \mathcal{Z}_n}{\prod_{s=0}^{n-1} \Omega_s^N} \right].$$

Applying Jensen’s inequality twice yields

$$\frac{d\Phi_0^N}{d\phi_0^y}(z_0) \geq \frac{N^n \mathcal{Z}_0 / \mathcal{Z}_n}{\int \vec{\mathbf{B}}_{1:n}(z_0, dz_{1:n}) \mathbb{E}_{z_{0:n}} \left[ \prod_{s=0}^{n-1} N^{-1} \Omega_s^N \right]},$$

and it then follows that

$$\mathsf{KL}(\phi_0^y \parallel \Phi_0^N) \leq \int \log \left( \frac{\mathcal{Z}_n}{\mathcal{Z}_0} \int \vec{\mathbf{B}}_{1:n}(z_0, dz_{1:n}) \mathbb{E}_{z_{0:n}} \left[ \prod_{s=0}^{n-1} N^{-1} \Omega_s^N \right] \right) \phi_0^y(dz_0).$$

Finally, using Lemma B.2 and the fact that  $\log(1 + x) < x$  for  $x > 0$  we get

$$\mathsf{KL}(\phi_0^y \parallel \Phi_0^N) \leq \frac{\mathsf{C}_{0:n}^y}{N-1} + \frac{\mathsf{D}_{0:n}^y}{N^2}$$

where

$$C_{0:n}^y := \sum_{s=1}^n \int \frac{\mathcal{Z}_s / \mathcal{Z}_0}{\bar{q}_{s|0}(\bar{z}_s|y)} \left( p_{0|s}(x_0|z_s) \delta_y(dx_0) dx_{\bar{0}} \right) \phi_s^y(dz_s),$$

and  $\phi_s^y(z_s) \propto p_s(z_s) \int p_{0|s}(z_0|z_s) \delta_y(dz_0) d\bar{z}_0$ .  $\square$

### Proof of Lemma B.1 and Lemma B.2.

*Proof of Lemma B.1.* We have that

$$\begin{aligned} & \Phi_{0:n}^N(dz_{0:n}) \\ &= N^{-1} \int P_{0:n}^N(dx_{0:n}^{1:N}, da_{1:n}^{1:N}) \sum_{k_{0:n} \in [1:N]^{n+1}} \delta_{y \sim \underline{x}_0^{k_0}}(dz_0) \prod_{s=1}^n \mathbb{1}\{k_s = a_s^{k_{s-1}}\} \delta_{x_s^{k_s}}(dz_s) \\ &= N^{-1} \int \sum_{k_{0:n}} \sum_{a_{1:n}^{1:N}} \delta_{y \sim \underline{x}_0^{k_0}}(dz_0) \prod_{s=1}^n \mathbb{1}\{k_s = a_s^{k_{s-1}}\} \delta_{x_s^{k_s}}(dz_s) \\ & \quad \times \prod_{j=1}^N p_n^y(dx_n^j) \left\{ \prod_{\ell=2}^n \prod_{i=1}^N \omega_{\ell-1}^{a_{\ell-1}^i} p_{\ell-1}^y(dx_{\ell-1}^i | x_{\ell}^{a_{\ell}^i}) \right\} \prod_{r=1}^N \omega_0^{a_r^r} p_{\ell-1}^y(dx_0^r | x_1^{a_1^r}) \delta_y(\bar{x}_0^r) \\ &= N^{-1} \int \sum_{k_{0:n}} \sum_{a_{1:n}^{1:N}} p_n^y(dx_n^{k_n}) \delta_{x_n^{k_n}}(dz_n) \prod_{j \neq k_n} p_n^y(dx_n^j) \prod_{\ell=2}^n \left\{ \prod_{i \neq k_{\ell-1}} \omega_{\ell-1}^{a_{\ell-1}^i} p_{\ell-1}^y(dx_{\ell-1}^i | x_{\ell}^{a_{\ell}^i}) \right. \\ & \quad \times \mathbb{1}\{a_{\ell}^{k_{\ell-1}} = k_{\ell}\} \frac{\tilde{\omega}_{\ell-1}(x_{\ell}^{a_{\ell}^{k_{\ell-1}}})}{\Omega_{\ell-1}^N} p_{\ell-1}^y(dx_{\ell}^{k_{\ell-1}} | x_{\ell}^{a_{\ell}^{k_{\ell-1}}}) \delta_{x_{\ell-1}^{k_{\ell-1}}}(dz_{\ell-1}) \left. \right\} \\ & \quad \times \left\{ \prod_{r \neq k_0} \omega_0^{a_r^r} p_0^y(dx_0^r | x_1^{a_1^r}) \delta_y(\bar{x}_0^r) \right\} \mathbb{1}\{a_1^{k_0} = k_1\} \frac{\tilde{\omega}_0(x_1^{a_1^{k_0}})}{\Omega_0^N} p_0^y(dx_0^{k_0} | x_0^{a_1^{k_0}}) \delta_{y \sim \underline{x}_0^{k_0}}(dz_0). \end{aligned}$$

Then, using that for all  $s \in [2:n]$

$$\tilde{\omega}_{s-1}(x_s^{k_s}) p_{s-1}^y(dx_{s-1}^{k_{s-1}} | x_s^{k_s}) = \frac{\bar{q}_{s-1|0}(\bar{x}_{s-1}^{k_{s-1}} | y)}{\bar{q}_{s|0}(\bar{x}_s^{k_s} | y)} p_s(dx_{s-1}^{k_{s-1}} | x_s^{k_s}),$$

we recursively get that

$$\begin{aligned} & p_n^y(dx_n^{k_n}) \delta_{x_n^{k_n}}(dz_n) \prod_{s=2}^n \mathbb{1}\{a_s^{k_{s-1}} = k_s\} \frac{\tilde{\omega}_{s-1}(x_s^{k_{s-1}})}{\Omega_{s-1}^N} p_{s-1}^y(dx_{s-1}^{k_{s-1}} | x_s^{k_{s-1}}) \delta_{x_{s-1}^{k_{s-1}}}(dz_{s-1}) \\ & \quad \times \mathbb{1}\{a_1^{k_0} = k_1\} \frac{\tilde{\omega}_0(x_1^{k_0})}{\Omega_0^N} p_0^y(dx_0^{k_0} | x_1^{k_0}) \delta_{y \sim \underline{x}_0^{k_0}}(dz_0) \\ &= \frac{\bar{q}_{n|0}(z_n | y) p_n(dz_n)}{\mathcal{Z}_n} \delta_{z_n}(dx_n^{k_n}) \prod_{s=2}^n \mathbb{1}\{a_s^{k_{s-1}} = k_s\} \frac{\bar{q}_{s-1|0}(\bar{z}_{s-1} | y)}{\Omega_{s-1}^N \bar{q}_{s|0}(\bar{z}_s | y)} p_{s-1}(dz_{s-1} | z_s) \delta_{z_{s-1}}(dx_{s-1}^{k_{s-1}}) \\ & \quad \times \mathbb{1}\{a_1^{k_0} = k_1\} \frac{\bar{p}_0(y | z_1)}{\Omega_0^N \bar{q}_{1|0}(\bar{z}_1 | y)} p_0(dz_0 | z_1) \delta_y(dz_0) \delta_{z_0}(dx_0^{k_0}) \\ &= \frac{\mathcal{Z}_0}{\mathcal{Z}_n} \phi_{0:n}^y(dz_{0:n}) \delta_{z_n}(dx_n^{k_n}) \prod_{s=1}^n \mathbb{1}\{a_s^{k_{s-1}} = k_s\} \frac{1}{\Omega_{s-1}^N} \delta_{z_{s-1}}(dx_{s-1}^{k_{s-1}}). \end{aligned}$$

Thus, we obtain

$$\begin{aligned}
\Phi_{0:n}^N(dz_{0:n}) &= N^{-1} \int \sum_{k_{0:n}} \sum_{a_{1:n}^{1:N}} \phi_{0:n}^y(dz_{0:n}) \frac{\mathcal{Z}_0/\mathcal{Z}_n}{\prod_{s=0}^{n-1} \Omega_s^N} \delta_{z_n}(dx_n^{k_n}) \prod_{j \neq k_n} p_n^y(dx_n^j) \\
&\quad \times \prod_{\ell=2}^n \mathbb{1}\{a_{\ell}^{k_{\ell-1}} = k_{\ell}\} \delta_{z_{\ell-1}}(dx_{\ell-1}^{k_{\ell-1}}) \prod_{i \neq k_{\ell-1}} \omega_{\ell-1}^{a_i^{\ell}} p_{\ell-1}^y(dx_{\ell-1}^i | x_{\ell}^{a_{\ell}^{\ell}}) \\
&\quad \times \mathbb{1}\{a_1^{k_0} = k_1\} \delta_{z_0}(dx_0^{k_0}) \prod_{i \neq k_0} \omega_0^{a_i^1} p_0^y(\underline{x}_0^i | x_1^{a_1^1}) \delta_y(d\bar{x}_0) \\
&= N^{-1} \sum_{k_{0:n}} \phi_{0:n}^y(dz_{0:n}) \mathbb{E}_{z_{0:n}}^{\mathcal{Z}_0/\mathcal{Z}_n} \left[ \frac{\mathcal{Z}_0/\mathcal{Z}_n}{\prod_{s=0}^{n-1} \Omega_s^N} \right],
\end{aligned}$$

where for all  $k_{0:n} \in [1:N]^{n+1}$   $\mathbb{E}_{z_{0:n}}^{k_{0:n}}$  denotes the expectation under the Markov kernel

$$\begin{aligned}
\mathbf{P}_{k_{0:n}}^N(dx_{0:n}^{1:N}, a_{1:n}^{1:N}) | z_{0:n} &= \delta_{z_n}(dx_n^{k_n}) \prod_{i \neq k_n} p_n^y(dx_n^i) \\
&\quad \times \prod_{\ell=2}^n \delta_{z_{\ell-1}}(dx_{\ell-1}^{k_{\ell-1}}) \delta_{k_{\ell}}(da_{\ell}^{k_{\ell-1}}) \prod_{j \neq k_{\ell-1}} \sum_{k=1}^N \omega_{\ell-1}^k \delta_k(da_{\ell}^j) p_{\ell-1}^y(dx_{\ell-1}^j | x_{\ell}^{a_{\ell}^{\ell}}) \\
&\quad \times \delta_{z_0}(dx_0^{k_0}) \delta_{k_1}(da_1^{k_0}) \prod_{j \neq k_0} \sum_{k=1}^N \omega_0^k \delta_k(da_1^j) p_0^y(dx_0^j | x_1^{a_1^1}) \delta_y(d\bar{x}_0).
\end{aligned}$$

Note however that for all  $(k_{0:n}, \ell_{0:n}) \in ([1:N]^{n+1})^2$ ,

$$\mathbb{E}_{z_{0:n}}^{\mathcal{Z}_0/\mathcal{Z}_n} \left[ \frac{1}{\prod_{s=0}^{n-1} \Omega_s^N} \right] = \mathbb{E}_{z_{0:n}}^{\ell_{0:n}} \left[ \frac{1}{\prod_{s=0}^{n-1} \Omega_s^N} \right]$$

and thus it follows that

$$\Phi_{0:n}^N(dz_{0:n}) = \mathbb{E}_{z_{0:n}} \left[ \frac{N^n \mathcal{Z}_0/\mathcal{Z}_n}{\prod_{s=0}^{n-1} \Omega_s^N} \right] \phi_{0:n}^y(dz_{0:n}). \quad (\text{B.8})$$

□

Denote by  $\{\mathcal{F}_s\}_{s=0}^n$  the filtration generated by a conditional particle cloud sampled from the kernel  $\mathbf{P}^N$  (B.4), i.e. for all  $\ell \in [0:n-1]$

$$\mathcal{F}_s = \sigma(\xi_{s:n}^{1:N}, I_{s+1:n}^{1:N}).$$

and  $\mathcal{F}_n = \sigma(\xi_n^{1:N})$ . Define for all bounded  $f$  and  $\ell \in [0:n-1]$

$$\gamma_{\ell:n}^N(f) = \left\{ \prod_{s=\ell+1}^{n-1} N^{-1} \Omega_s^N \right\} N^{-1} \sum_{k=1}^N \tilde{\omega}_{\ell}(\xi_{\ell+1}^k) f(\xi_{\ell+1}^k), \quad (\text{B.9})$$

with the convention  $\gamma_{\ell:n}^N(f) = 1$  if  $\ell \geq n$ . Define also the transition Kernel

$$Q_{\ell-1|\ell+1}^y : \mathbb{R}^{\mathbf{d}_x} \times \mathcal{B}(\mathbb{R}^{\mathbf{d}_x}) \ni (x_{\ell+1}, A) \mapsto \int \mathbb{1}_A(x_{\ell}) \tilde{\omega}_{\ell-1}(x_{\ell}) p_{\ell}^y(dx_{\ell} | x_{\ell+1}). \quad (\text{B.10})$$

Using eqs. (2.3) and (2.4), it is easily seen that for all  $\ell \in [0:n-1]$ ,

$$\tilde{\omega}_{\ell}(x_{\ell+1}) Q_{\ell-1|\ell+1}^y(f)(x_{\ell+1}) = \frac{1}{\bar{q}_{\ell+1|0}(\bar{x}_{\ell+1}|y)} \int \bar{q}_{\ell|0}(\bar{x}_s|y) \tilde{\omega}_{\ell-1}(x_{\ell}) f(x_{\ell}) p_{\ell}(dx_{\ell} | x_{\ell+1}). \quad (\text{B.11})$$

Define  $\mathbf{1} : x \in \mathbb{R}^{\mathbf{d}_x} \mapsto 1$ . We may thus write that  $\gamma_{\ell:n}^N(f) = N^{-1} \gamma_{\ell+1:n}^N(\mathbf{1}) \sum_{k=1}^N \tilde{\omega}_{\ell}(\xi_{\ell+1}^k) f(\xi_{\ell+1}^k)$ .

**Lemma B.3.** *For all  $\ell \in [0 : n - 1]$  it holds that*

$$\mathbb{E}_{z_{0:n}} [\gamma_{\ell-1:n}^N(f)] = \frac{N-1}{N} \mathbb{E}_{z_{0:n}} [\gamma_{\ell:n}^N(Q_{\ell-1|\ell+1}^y(f))] + \frac{1}{N} \mathbb{E}_{z_{0:n}} [\gamma_{\ell:n}^N(\mathbf{1})] \tilde{\omega}_{\ell-1}(z_\ell) f(z_\ell).$$

*Proof.* By the tower property and the fact that  $\gamma_{\ell:n}^N(f)$  is  $\mathcal{F}_{\ell+1}$ -measurable, we have that

$$\mathbb{E}_{z_{0:n}} [\gamma_{\ell-1:n}^N(f)] = \mathbb{E}_{z_{0:n}} \left[ N^{-1} \gamma_{\ell+1:n}^N(\mathbf{1}) \Omega_\ell^N \mathbb{E}_{z_{0:n}} \left[ N^{-1} \sum_{k=1}^N \tilde{\omega}_{\ell-1}(\xi_\ell^k) f(\xi_\ell^k) \middle| \mathcal{F}_{\ell+1} \right] \right].$$

Note that for all  $\ell \in [0 : n - 1]$ ,  $(\xi_\ell^1, \dots, \xi_\ell^{N-1})$  are identically distributed conditionally on  $\mathcal{F}_{\ell+1}$  and

$$\mathbb{E}_{z_{0:n}} \left[ \tilde{\omega}_{\ell-1}(\xi_\ell^j) f(\xi_\ell^j) \middle| \mathcal{F}_{\ell+1} \right] = \frac{1}{\Omega_\ell^N} \sum_{k=1}^N \tilde{\omega}_\ell(\xi_{\ell+1}^k) \int \tilde{\omega}_{\ell-1}(x_\ell) f(x_\ell) p_\ell^y(dx_\ell | \xi_{\ell+1}^k),$$

leading to

$$\begin{aligned} \mathbb{E}_{z_{0:n}} \left[ N^{-1} \sum_{k=1}^N \tilde{\omega}_{\ell-1}(\xi_\ell^k) f(\xi_\ell^k) \middle| \mathcal{F}_{\ell+1} \right] \\ = \frac{N-1}{N \Omega_\ell^N} \sum_{k=1}^N \tilde{\omega}_\ell(\xi_{\ell+1}^k) \int \tilde{\omega}_{\ell-1}(x_\ell) f(x_\ell) p_\ell^y(dx_\ell | \xi_{\ell+1}^k) + \frac{1}{N} \tilde{\omega}_{\ell-1}(z_\ell) f(z_\ell), \end{aligned}$$

and the desired recursion follows.  $\square$

*Proof of Lemma B.2.* We proceed by induction and show for all  $\ell \in [0 : n - 2]$

$$\begin{aligned} \mathbb{E}_{z_{0:n}} [\gamma_{\ell:n}^N(f)] \\ = \left( \frac{N-1}{N} \right)^{n-\ell} \frac{\int p_{\ell+1}(dx_{\ell+1}) \bar{q}_{\ell+1|0}(\bar{x}_{\ell+1}|y) \tilde{\omega}_\ell(x_{\ell+1}) f(x_{\ell+1})}{\mathcal{Z}_n} \\ + \frac{(N-1)^{n-\ell-1}}{N^{n-\ell}} \left[ (\mathcal{Z}_{\ell+1}/\mathcal{Z}_n) f(z_{\ell+1}) \tilde{\omega}_\ell(z_{\ell+1}) \right. \\ \left. + \sum_{s=\ell+2}^n \frac{\mathcal{Z}_s/\mathcal{Z}_n}{\bar{q}_{s|0}(\bar{z}_s|y)} \int \tilde{\omega}_\ell(x_{\ell+1}) \bar{q}_{\ell+1|0}(\bar{x}_{\ell+1}|y) f(x_{\ell+1}) p_{\ell+1|s}(dx_{\ell+1}|z_s) \right] + \frac{D_{\ell:n}^y}{N^2}. \end{aligned} \tag{B.12}$$

where  $f$  is a bounded function and  $D_{\ell:n}^y$  is a positive constant. The desired result in Lemma B.2 then follows by taking  $\ell = 0$  and  $f = \mathbf{1}$ .

Assume that (B.12) holds at step  $\ell$ . To show that it holds at step  $\ell - 1$  we use Lemma B.3 and we compute  $\mathbb{E}_{z_{0:n}} [\gamma_{\ell:n}^N(Q_{\ell-1|\ell+1}^y(f))]$  and  $\mathbb{E}_{z_{0:n}} [\gamma_{\ell:n}^N(\mathbf{1})] \tilde{\omega}_{\ell-1}(z_\ell) f(z_\ell)$ .

Using the following identities which follow from (B.11)

$$\begin{aligned} \int \bar{q}_{\ell+1|0}(\bar{x}_{\ell+1}|y) \tilde{\omega}_\ell(x_{\ell+1}) Q_{\ell-1|\ell+1}^y(f)(x_{\ell+1}) p_{\ell+1}(dx_{\ell+1}) \\ = \int \bar{q}_{\ell|0}(\bar{x}_\ell|y) \tilde{\omega}_{\ell-1}(x_\ell) f(x_\ell) p_\ell(dx_\ell), \end{aligned}$$

and

$$\begin{aligned} \int \tilde{\omega}_\ell(x_{\ell+1}) \bar{q}_{\ell+1|0}(\bar{x}_{\ell+1}|y) Q_{\ell-1|\ell+1}^y(f)(x_{\ell+1}) p_{\ell+1|s}(dx_{\ell+1}|x_s) \\ = \int \tilde{\omega}_{\ell-1}(x_\ell) \bar{q}_{\ell|0}(\bar{x}_\ell|y) f(x_\ell) p_{\ell|s}(dx_\ell|x_s), \end{aligned}$$

we get by (B.12) that

$$\begin{aligned}
& \frac{N-1}{N} \mathbb{E}_{z_{0:n}} [\gamma_{\ell:n}^N (Q_{\ell-1|\ell+1}^y(f))] \\
&= \left( \frac{N-1}{N} \right)^{n-\ell+1} \frac{\int \bar{q}_{\ell|0}(\bar{x}_\ell|y) \tilde{\omega}_{\ell-1}(x_\ell) f(x_\ell) \mathbf{p}_\ell(dx_\ell)}{\mathcal{Z}_n} \\
&+ \frac{(N-1)^{n-\ell}}{N^{n-\ell+1}} \left[ \frac{\mathcal{Z}_{\ell+1}/\mathcal{Z}_n}{\bar{q}_{\ell+1|0}(\bar{z}_{\ell+1}|y)} \int \bar{q}_{\ell|0}(\bar{x}_\ell|y) \tilde{\omega}_{\ell-1}(x_\ell) f(x_\ell) p_\ell(dx_\ell|z_{\ell+1}) \right. \\
&\quad \left. + \sum_{s=\ell+2}^n \frac{\mathcal{Z}_s/\mathcal{Z}_n}{\bar{q}_{s|0}(\bar{z}_s|y)} \int \tilde{\omega}_{\ell-1}(x_\ell) \bar{q}_{\ell|0}(\bar{x}_\ell|y) f(x_\ell) p_{\ell|s}(dx_\ell|z_s) \right] + \frac{\mathbf{D}_{\ell:n}^y}{N^2} \\
&= \left( \frac{N-1}{N} \right)^{n-\ell+1} \frac{\int \bar{q}_{\ell|0}(\bar{x}_\ell|y) \tilde{\omega}_{\ell-1}(x_\ell) f(x_\ell) \mathbf{p}_\ell(dx_\ell)}{\mathcal{Z}_n} \\
&+ \frac{(N-1)^{n-\ell}}{N^{n-\ell+1}} \sum_{s=\ell+1}^n \frac{\mathcal{Z}_s/\mathcal{Z}_n}{\bar{q}_{s|0}(\bar{z}_s|y)} \int \tilde{\omega}_{\ell-1}(x_\ell) \bar{q}_{\ell|0}(\bar{x}_s|y) f(x_\ell) p_{\ell|s}(dx_\ell|z_s) + \frac{\mathbf{D}_{\ell:n}^y}{N^2}. \tag{B.13}
\end{aligned}$$

The induction step is finished by using again (B.12) and noting that

$$\frac{1}{N} \mathbb{E}_{z_{0:n}} [\gamma_{\ell:n}^N(\mathbf{1})] \tilde{\omega}_{\ell-1}(z_\ell) f(z_\ell) = \frac{(N-1)^{n-\ell}}{N^{n-\ell+1}} (\mathcal{Z}_\ell/\mathcal{Z}_n) \tilde{\omega}_{\ell-1}(z_\ell) f(z_\ell) + \frac{\tilde{\mathbf{D}}_{\ell:n}^y}{N^2}.$$

and then setting  $\mathbf{D}_{\ell-1:n}^y = \mathbf{D}_{\ell:n}^y + \tilde{\mathbf{D}}_{\ell:n}^y$ .

It remains to compute the initial value at  $\ell = n-2$ . Note that

$$\mathbb{E}_{z_{0:n}} [\gamma_{n-2:n}^N(f)] = \frac{N-1}{N} \int p_n^y(dx_n) \tilde{\omega}_{n-1}(x_n) f(x_n) + \frac{1}{N} \tilde{\omega}_{n-1}(z_n) f(z_n) \tag{B.14}$$

and thus by Lemma B.3 and similarly to the previous computations

$$\begin{aligned}
& \mathbb{E}_{z_{0:n}} [\gamma_{n-2:n}^N(f)] \\
&= \left( \frac{N-1}{N} \right)^2 \int p_n^y(dx_n) \tilde{\omega}_{n-1}(x_n) Q_{n-2|n}^y(f)(x_n) + \frac{N-1}{N^2} \left[ \tilde{\omega}_{n-1}(z_n) Q_{n-2|n}^y(f)(z_n) \right. \\
&\quad \left. + \tilde{\omega}_{n-2}(z_{n-1}) f(z_{n-1}) \int p_n^y(dx_n) \tilde{\omega}_{n-1|n}(x_n) \right] + \frac{\mathbf{D}_{n-2fa:n}^y}{N^2} \\
&= \left( \frac{N-1}{N} \right)^2 \frac{\int \bar{q}_{n-1|0}(x_{n-1}|y) \tilde{\omega}_{n-2}(x_{n-1}) \mathbf{p}_{n-1}(dx_{n-1})}{\mathcal{Z}_n} \\
&+ \frac{N-1}{N^2} \left[ (\mathcal{Z}_{n-1}/\mathcal{Z}_n) \tilde{\omega}_{n-2}(z_{n-1}) f(z_{n-1}) \right. \\
&\quad \left. + \frac{1}{\bar{q}_{n|0}(\bar{x}_n|y)} \int \bar{q}_{n-1|0}(\bar{x}_{n-1}|y) \tilde{\omega}_{n-2}(x_{n-1}) f(x_{n-1}) p_{n-1}(dx_{n-1}|z_n) \right] + \frac{\mathbf{D}_{n-2:n}^y}{N^2}.
\end{aligned}$$

□

**B.2. Proof of Proposition 2.3 and Lemma B.4.** In this section and only in this section we make the following assumption

**(A2)** For all  $s \in [0 : n-1]$ ,  $\mathbf{p}_s(x_s) q_{s+1}(x_{s+1}|x_s) = \mathbf{p}_{s+1}(x_{s+1}) \lambda_s(x_s|x_{s+1})$ .

We also consider  $\sigma_\delta = 0$ . In what follows we let  $\tau_{d_y+1} = n$  and we write  $\tau_{1:d_y} = \{\tau_1, \dots, \tau_{d_y}\}$  and  $\overline{\tau_{1:d_y}} = [1:n] \setminus \tau_{1:t}$ . Define the measure

$$\Gamma_{0:n}^y(d\mathbf{x}_{0:n}) = \mathfrak{p}_n(d\mathbf{x}_n) \prod_{s \in \overline{\tau_{1:d_y}}} \lambda_s(d\mathbf{x}_s | \mathbf{x}_{s+1}) \prod_{i=1}^{d_y} \lambda_{\tau_i}(\mathbf{x}_{\tau_i} | \mathbf{x}_{\tau_i+1}) d\mathbf{x}_{\tau_i}^{\setminus i} \delta_{\mathbf{y}[i]}(d\mathbf{x}_{\tau_i}[i]). \quad (\text{B.15})$$

Under (A2) it has the following alternative *forward* expression,

$$\Gamma_{0:n}^y(d\mathbf{x}_{0:n}) = \mathfrak{p}_0(d\mathbf{x}_0) \prod_{s \in \overline{\tau_{1:d_y}}} q_{s+1}(\mathbf{x}_{s+1} | \mathbf{x}_s) \prod_{i=1}^{d_y} q_{\tau_i}(\mathbf{x}_{\tau_i} | \mathbf{x}_{\tau_i-1}) d\mathbf{x}_{\tau_i}^{\setminus i} \delta_{\mathbf{y}[i]}(d\mathbf{x}_{\tau_i}[i]). \quad (\text{B.16})$$

Since the forward kernels decompose over the dimensions of the states, i.e.

$$q_{s+1}(\mathbf{x}_{s+1} | \mathbf{x}_s) = \prod_{\ell=1}^{d_x} q_{s+1}^\ell(\mathbf{x}_{s+1}[\ell] | \mathbf{x}_s[\ell])$$

where  $q_{s+1}^\ell(\mathbf{x}_{s+1}[\ell] | \mathbf{x}_s[\ell]) = \mathcal{N}(\mathbf{x}_{s+1}[\ell]; (\alpha_{s+1}/\alpha_s)^{1/2} \mathbf{x}_s[\ell], 1 - (\alpha_{s+1}/\alpha_s))$ , we can write

$$\Gamma_{0:n}^y(\mathbf{x}_{0:n}) = \mathfrak{p}_0(\mathbf{x}_0) \prod_{\ell=1}^{d_x} \Gamma_{1:n|0,\ell}^y(\mathbf{x}_1[\ell], \dots, \mathbf{x}_n[\ell] | \mathbf{x}_0[\ell]), \quad (\text{B.17})$$

where for  $\ell \in [1 : d_y]$

$$\Gamma_{1:n|0,\ell}^y(\mathbf{x}_1[\ell], \dots, \mathbf{x}_n[\ell] | \mathbf{x}_0[\ell]) = q_{\tau_\ell}^\ell(\mathbf{y}[\ell] | \mathbf{x}_{\tau_\ell-1}[\ell]) \prod_{s \neq \tau_\ell} q_s^\ell(d\mathbf{x}_s[\ell] | \mathbf{x}_{s-1}[\ell]), \quad (\text{B.18})$$

and for  $\ell \in [d_y + 1 : d_x]$ ,

$$\Gamma_{1:n|0,\ell}^y(\mathbf{x}_1[\ell], \dots, \mathbf{x}_n[\ell] | \mathbf{x}_0[\ell]) = \prod_{s=0}^{n-1} q_{s+1}^\ell(\mathbf{x}_{s+1}[\ell] | \mathbf{x}_s[\ell]). \quad (\text{B.19})$$

With these quantities in hand we can now prove Proposition 2.3.

*Proof of Proposition 2.3.* Note that for  $\ell \in [1 : d_y]$ ,

$$\begin{aligned} \mathcal{N}(\mathbf{y}[\ell]; \alpha_{\tau_\ell} \mathbf{x}_0[\ell], 1 - \alpha_{\tau_\ell}) &= q_{\tau_\ell|0}^\ell(\mathbf{y}[\ell] | \mathbf{x}_0[\ell]) = \int q_{\tau_\ell}^\ell(\mathbf{y}[\ell] | \mathbf{x}_{\tau_\ell-1}[\ell]) \prod_{s \neq \tau_\ell} q_s^\ell(d\mathbf{x}_s[\ell] | \mathbf{x}_{s-1}[\ell]) \\ &= \int \Gamma_{1:n|0,\ell}^y(d(\mathbf{x}_1[\ell], \dots, \mathbf{x}_n[\ell]) | \mathbf{x}_0[\ell]) \end{aligned}$$

and thus by (??) we have that

$$\begin{aligned} \mathfrak{p}_0(\mathbf{x}_0) g_0^y(\mathbf{x}_0) &\propto \mathfrak{p}_0(\mathbf{x}_0) \prod_{\ell=1}^{d_y} \mathcal{N}(\mathbf{y}[\ell]; \alpha_{\tau_\ell} \mathbf{x}_0[\ell], 1 - \alpha_{\tau_\ell}) \\ &= \mathfrak{p}_0(\mathbf{x}_0) \prod_{\ell=1}^{d_y} \int \Gamma_{1:n|0,\ell}^y(d(\mathbf{x}_1[\ell], \dots, \mathbf{x}_n[\ell]) | \mathbf{x}_0[\ell]) \\ &= \mathfrak{p}_0(\mathbf{x}_0) \prod_{\ell=1}^{d_x} \int \Gamma_{1:n|0,\ell}^y(d(\mathbf{x}_1[\ell], \dots, \mathbf{x}_n[\ell]) | \mathbf{x}_0[\ell]). \end{aligned}$$

By (B.16) it follows that

$$\phi_0^y(\mathbf{x}_0) = \frac{1}{\int \Gamma_{0:n}^y(\tilde{\mathbf{x}}_{0:n}) d\tilde{\mathbf{x}}_{0:n}} \int \Gamma_{0:n}^y(\mathbf{x}_{0:n}) d\mathbf{x}_{1:n},$$

and hence by (B.16) and (B.15) we get

$$\phi_0^{\mathbf{y}}(\mathbf{x}_0) \propto \int \mathfrak{p}_{\tau_{d_y}}(\mathbf{x}_{\tau_{d_y}}) \delta_{\mathbf{y}[d_y]}(d\mathbf{x}_{\tau_{d_y}}[d_y]) d\mathbf{x}_{\tau_{d_y}}^{\setminus d_y} \left\{ \prod_{i=1}^{d_y-1} \lambda_{\tau_i|\tau_{i+1}}(\mathbf{x}_{\tau_i}|\mathbf{x}_{\tau_{i+1}}) \delta_{\mathbf{y}[i]}(d\mathbf{x}_{\tau_i}[i]) d\mathbf{x}_{\tau_i}^{\setminus i} \right\} \lambda_{0|\tau_1}(\mathbf{x}_0|\mathbf{x}_{\tau_1}).$$

This completes the proof.  $\square$

Let  $\gamma_{0,s}^{\mathbf{y}}$  denote the joint time 0 and  $s$  marginal of the measure (B.15), i.e.

$$\gamma_{0,s}^{\mathbf{y}}(\mathbf{x}_0, \mathbf{x}_s) = \int \Gamma_{0:n}^{\mathbf{y}}(\mathbf{x}_{0:n}) d\mathbf{x}_{1:s-1} d\mathbf{x}_{s+1:n} \quad (\text{B.20})$$

We now prove the following result.

**Lemma B.4.** *Assume (A2) and let  $\tau_0 := 0$ ,  $\tau_{d_y+1} := n$ . For all  $k \in [1 : d_y]$ ,*

(i) *If  $s \in [\tau_k + 1 : \tau_{k+1}]$ ,*

$$\gamma_{0,s}^{\mathbf{y}}(\mathbf{x}_0, \mathbf{x}_s) = \int \gamma_{0,s+1}^{\mathbf{y}}(\mathbf{x}_0, \mathbf{x}_{s+1}) \underline{q}_{s|s+1,0}^{\sigma}(\underline{x}_s|\underline{x}_{s+1}, \underline{x}_0) g_s^{\mathbf{y}}(\bar{x}_s) \prod_{\ell=k+1}^{d_y} q_{s|s+1,0}^{\sigma,\ell}(\mathbf{x}_s[\ell]|\mathbf{x}_{s+1}[\ell], \mathbf{x}_0[\ell]) d\mathbf{x}_{s+1}.$$

(ii) *If  $s = \tau_k$ ,*

$$\begin{aligned} \gamma_{0,s}^{\mathbf{y}}(\mathbf{x}_0, \mathbf{x}_s) &= \int \gamma_{0,s+1}^{\mathbf{y}}(\mathbf{x}_0, \mathbf{x}_{s+1}) \underline{q}_{s|s+1,0}^{\sigma}(\underline{x}_s|\underline{x}_{s+1}, \underline{x}_0) \\ &\quad \times \prod_{i=1}^{k-1} g_{s,i}^{\mathbf{y}}(\bar{x}_s[i]) \prod_{\ell=k+1}^{d_y} q_{s|s+1,0}^{\sigma,\ell}(\mathbf{x}_s[\ell]|\mathbf{x}_{s+1}[\ell], \mathbf{x}_0[\ell]) d\mathbf{x}_{s+1}. \end{aligned}$$

*Proof of Lemma B.4.* Let  $k \in [1 : d_y]$  and assume that  $s \in [\tau_k + 1 : \tau_{k+1} - 2]$ . By (A2), (B.16), (B.18) and (B.19) we have that

$$\begin{aligned} \gamma_{0,s}^{\mathbf{y}}(\mathbf{x}_0, \mathbf{x}_s) &= \mathfrak{p}_0(\mathbf{x}_0) \underline{q}_{s|0}(\underline{x}_s|\underline{x}_0) \prod_{i=1}^k q_{\tau_i|0}^i(\mathbf{y}[i]|\mathbf{x}_0[i]) q_{s|\tau_i}^i(\mathbf{x}_s[i]|\mathbf{y}[i]) \\ &\quad \times \prod_{\ell=k+1}^{d_y} q_{s|0}^{\ell}(\mathbf{x}_s[\ell]|\mathbf{x}_0[\ell]) q_{\tau_{\ell}|s}^{\ell}(\mathbf{y}[\ell]|\mathbf{x}_s[\ell]), \end{aligned}$$

and thus, using the following identity valid for  $\ell \in [k+1 : d_y]$

$$\begin{aligned} q_{s|0}^{\ell}(\mathbf{x}_s[\ell]|\mathbf{x}_0[\ell]) q_{\tau_{\ell}|s}^{\ell}(\mathbf{y}[\ell]|\mathbf{x}_s[\ell]) \\ &= q_{s|0}^{\ell}(\mathbf{x}_s[\ell]|\mathbf{x}_0[\ell]) \int q_{\tau_{\ell}|s+1}^{\ell}(\mathbf{y}[\ell]|\mathbf{x}_{s+1}[\ell]) q_{s+1}^{\ell}(\mathbf{x}_{s+1}[\ell]|\mathbf{x}_s[\ell]) d\mathbf{x}_{s+1}[\ell] \\ &= \int q_{s|s+1,0}^{\sigma,\ell}(\mathbf{x}_s[\ell]|\mathbf{x}_{s+1}[\ell], \mathbf{x}_0[\ell]) q_{\tau_{\ell}|s+1}^{\ell}(\mathbf{y}[\ell]|\mathbf{x}_{s+1}[\ell]) q_{s+1|0}^{\ell}(\mathbf{x}_{s+1}[\ell]|\mathbf{x}_0[\ell]) d\mathbf{x}_{s+1}[\ell], \end{aligned}$$

and that  $\underline{q}_{s|0}(\underline{x}_s|x_0)\underline{q}_{s+1}(\underline{x}_{s+1}|\underline{x}_s) = \underline{q}_{s|s+1,0}^\sigma(\underline{x}_s|\underline{x}_{s+1},\underline{x}_0)\underline{q}_{s+1|0}(\underline{x}_{s+1}|\underline{x}_0)$  we get that

$$\begin{aligned} & \gamma_{0,s}^{\mathbf{y}}(\mathbf{x}_0, \mathbf{x}_s) \\ &= \int \mathbf{p}_0(\mathbf{x}_0) \underline{q}_{s|0}(\underline{x}_s|x_0) \underline{q}_{s+1}(\mathrm{d}\underline{x}_{s+1}|\underline{x}_s) \\ & \quad \times \prod_{i=1}^k q_{\tau_i|0}^i(\mathbf{y}[i]|\mathbf{x}_0[i]) q_{s|\tau_i}^i(\mathbf{x}_s[i]|\mathbf{y}[i]) q_{s+1|\tau_i}^i(\mathrm{d}\mathbf{x}_{s+1}[i]|\mathbf{y}[i]) \\ & \quad \times \prod_{\ell=k+1}^{d_y} q_{s|s+1,0}^{\sigma,\ell}(\mathbf{x}_s[\ell]|\mathbf{x}_{s+1}[\ell], \mathbf{x}_0[\ell]) q_{\tau_\ell|s+1}^\ell(\mathbf{y}[\ell]|\mathbf{x}_{s+1}[\ell]) q_{s+1|0}^\ell(\mathbf{x}_{s+1}[\ell]|\mathbf{x}_0[\ell]) \mathrm{d}\mathbf{x}_{s+1}[\ell] \\ &= \int \gamma_{0,s+1}^{\mathbf{y}}(\mathbf{x}_0, \mathbf{x}_{s+1}) \underline{q}_{s|s+1,0}^\sigma(\underline{x}_s|\underline{x}_{s+1}, \underline{x}_0) g_s^{\mathbf{y}}(\bar{x}_s) \prod_{\ell=k+1}^{d_y} q_{s|s+1,0}^{\sigma,\ell}(\mathbf{x}_s[\ell]|\mathbf{x}_{s+1}[\ell], \mathbf{x}_0[\ell]) \mathrm{d}\mathbf{x}_{s+1}. \end{aligned}$$

If  $s = \tau_{k+1}$  then

$$\begin{aligned} \gamma_{0,s}^{\mathbf{y}}(\mathbf{x}_0, \mathbf{x}_s) &= \mathbf{p}_0(\mathbf{x}_0) \underline{q}_{s|0}(\underline{x}_s|x_0) \prod_{i=1}^k q_{\tau_i|0}^i(\mathbf{y}[i]|\mathbf{x}_0[i]) q_{s|\tau_i}^i(\mathbf{x}_s[i]|\mathbf{y}[i]) \\ & \quad \times q_{\tau_{k+1}|0}^{k+1}(\mathbf{y}[k+1]|\mathbf{x}_0[k+1]) \prod_{\ell=k+2}^{d_y} q_{s|0}^\ell(\mathbf{x}_s[\ell]|\mathbf{x}_0[\ell]) q_{\tau_\ell|s}^\ell(\mathbf{y}[\ell]|\mathbf{x}_s[\ell]), \end{aligned} \tag{B.21}$$

and similarly to the previous case we get

$$\begin{aligned} & \gamma_{0,s}(\mathbf{x}_0, \mathbf{x}_s) \\ &= \int \gamma_{0,s+1}^{\mathbf{y}}(\mathbf{x}_0, \mathbf{x}_{s+1}) \underline{q}_{s|s+1,0}^\sigma(\underline{x}_s|\underline{x}_{s+1}, \underline{x}_0) g_s^{\mathbf{y}}(\bar{x}_s) \prod_{\ell=k+2}^{d_y} q_{s|s+1,0}^{\sigma,\ell}(\mathbf{x}_s[\ell]|\mathbf{x}_{s+1}[\ell], \mathbf{x}_0[\ell]) \mathrm{d}\mathbf{x}_{s+1}. \end{aligned}$$

Finally, if  $s = \tau_{k+1} - 1$ , then

$$\begin{aligned} \gamma_{0,s}^{\mathbf{y}}(\mathbf{x}_0, \mathbf{x}_s) &= \mathbf{p}_0(\mathbf{x}_0) \underline{q}_{s|0}(\underline{x}_s|x_0) \prod_{i=1}^k q_{\tau_i|0}^i(\mathbf{y}[i]|\mathbf{x}_0[i]) q_{s|\tau_i}^i(\mathbf{x}_s[i]|\mathbf{y}[i]) \\ & \quad \times q_{s|0}^{k+1}(\mathbf{x}_s[k+1]|\mathbf{x}_0[k+1]) q_{\tau_{k+1}|s}^{k+1}(\mathbf{y}[k+1]|\mathbf{x}_s[k+1]) \prod_{\ell=k+2}^{d_y} q_{s|0}^\ell(\mathbf{x}_s[\ell]|\mathbf{x}_0[\ell]) q_{\tau_\ell|s}^\ell(\mathbf{y}[\ell]|\mathbf{x}_s[\ell]), \end{aligned}$$

and using

$$\begin{aligned} & q_{s|0}^{k+1}(\mathbf{x}_s[k+1]|\mathbf{x}_0[k+1]) q_{\tau_{k+1}|s}^{k+1}(\mathbf{y}[k+1]|\mathbf{x}_s[k+1]) \\ &= q_{s|\tau_{k+1},0}^{\sigma,k+1}(\mathbf{x}_s[k+1]|\mathbf{x}_{\tau_{k+1}}[k+1], \mathbf{x}_0[k+1]) q_{\tau_{k+1}|0}^{k+1}(\mathbf{y}[k+1]|\mathbf{x}_0[k+1]) \end{aligned}$$

we find that

$$\begin{aligned} & \gamma_{0,s}(\mathbf{x}_0, \mathbf{x}_s) \\ &= \int \gamma_{0,\tau_{k+1}}^{\mathbf{y}}(\mathbf{x}_0, \mathbf{x}_{\tau_{k+1}}) \underline{q}_{s|\tau_{k+1},0}^\sigma(\underline{x}_s|\underline{x}_{\tau_{k+1}}, \underline{x}_0) g_s^{\mathbf{y}}(\bar{x}_s) \prod_{\ell=k+1}^{d_y} q_{s|s+1,0}^{\sigma,\ell}(\mathbf{x}_s[\ell]|\mathbf{x}_{\tau_{k+1}}[\ell], \mathbf{x}_0[\ell]) \mathrm{d}\mathbf{x}_{\tau_{k+1}}. \end{aligned}$$

□

**B.3. Algorithmic details and numerics.** The code for both experiments is available at <https://anonymous.4open.science/r/mcgdiff/README.md>.

B.3.1. *GMM*. For a given dimension  $d_x$ , we consider  $q_{\text{data}}$  a mixture of 25 Gaussian random variables. The components have mean  $\mu_{i,j} := (8i, 8j, \dots, 8i, 8j) \in \mathbb{R}^{d_x}$  for  $(i, j) \in \{-2, -1, 0, 1, 2\}^2$  and unit variance. The associated unnormalized weights  $\omega_{i,j}$  are independently drawn according to a  $\chi^2$  distribution. We have set  $\sigma_\delta^2 = 10^{-4}$ .

Score. Note that  $q_s(x_s) = \int q_{s|0}(x_s|x_0)q_{\text{data}}(x_0)dx_0$ . As  $q_{\text{data}}$  is a mixture of Gaussians,  $q_s(x_s)$  is also a mixture of Gaussians with means  $\alpha_s^{1/2}\mu_{i,j}$  and unitary variances. Therefore, using automatic differentiation libraries, we can calculate  $\nabla \log q_s(x_s)$ . Setting  $e(x_s, s) = -(1 - \alpha_s)^{1/2}\nabla \log q_s(x_s)$  leads to the optimum of (1.9).

Forward process scaling. We chose the sequence of  $\{\beta_s\}_{s=1}^{1000}$  as a linearly decreasing sequence between  $\beta_1 = 0.2$  and  $\beta_{1000} = 10^{-4}$ .

Measurement model. For a pair of dimensions  $(d_x, d_y)$  the measurement model  $(y, A, \sigma_y)$  is drawn as follows:

- A: We first draw  $\tilde{A} \sim \mathcal{N}(0_{d_y \times d_x}, I_{d_y \times d_x})$  and compute the SVD decomposition of  $\tilde{A} = USV^T$ . Then, we sample for  $(i, j) \in \{-2, -1, 0, 1, 2\}^2$ ,  $s_{i,j}$  according to a uniform in  $[0, 1]$ . Finally, we set  $A = U \text{Diag}(\{s_{i,j}\}_{(i,j) \in \{-2, -1, 0, 1, 2\}^2})V^T$ .
- $\sigma_y$ : We draw  $\sigma_y$  uniformly in the interval  $[0, \max(s_1, \dots, s_{d_y})]$ .
- $y$ : We then draw  $x_* \sim q_{\text{data}}$  and set  $y := Ax_* + \sigma_y \epsilon$  where  $\epsilon \sim \mathcal{N}(0_{d_y}, I_{d_y})$ .

Posterior. Once we have drawn both  $q_{\text{data}}$  and  $(y, A, \sigma_y)$ , the posterior can be exactly calculated using Bayes formula and gives a mixture of Gaussians with mixture components  $c_{i,j}$  and associated weights  $\tilde{\omega}_{i,j}$

$$c_{i,j} := \mathcal{N}(\Sigma (A^T y / \sigma_y^2 + \mu_{i,j}), \Sigma),$$

$$\tilde{\omega}_i := \omega_i \mathcal{N}(y; A\mu_{i,j}, \sigma^2 I_{d_x} + AA^T),$$

where  $\Sigma := (I_{d_x} + \sigma_y^{-2} A^T A)^{-1}$ .

Choosing DDIM timesteps for a given measurement model. Given a number of DDIM samples  $R$ , we choose the timesteps  $1 = t_1 < \dots < t_R = 1000 \in [1 : 1000]$  as to try to satisfy the two following constraints:

- For all  $i \in [1 : d_y]$  there exists a  $t_j$  such that  $\sigma_y \alpha_{t_j}^{1/2} \approx (1 - \alpha_{t_j})^{1/2} s_i$ ,
- For all  $i \in [1 : R - 1]$ ,  $\alpha_{t_i}^{1/2} - \alpha_{t_{i+1}}^{1/2} \approx \delta$  for some  $\delta > 0$ .

The first constraint comes naturally from the definition of  $\tau_i$ . Since the potentials have mean  $\alpha_{t_i}^{1/2} y$ , the second condition constrains the intermediate laws remain “close”. An algorithm that approximately satisfies both constraints is given below.

---

**Algorithm 2:** Timesteps choice

---

**Input:** Number of DDIM steps  $R$ ,  $\sigma_y$ ,  $\{s_i\}_{i=1}^{d_y}$ ,  $\{\alpha_i\}_{i=1}^{1000}$

**Output:**  $\{t_j\}_{j=1}^R$

Set  $S_\tau = \{\}$ .

**for**  $j \leftarrow [1 : d_y]$  **do**

Set  $\tilde{\tau}_j = \text{argmin}_{\ell \in [1:1000]} |\sigma_y \alpha_\ell^{1/2} - (1 - \alpha_\ell)^{1/2} s_j|$ .  
Add  $\tilde{\tau}_j$  to  $S_\tau$  if  $\tilde{\tau}_j \notin S_\tau$ .

Set  $n_m = R - \#S_\tau - 1$  and  $\delta = (\alpha_1^{1/2} - \alpha_{1000}^{1/2})/n_m$ .

Set  $t_1 = 1$ ,  $e = 1$  and  $i_e = 1$ . **for**  $\ell \leftarrow [2 : 1000]$  **do**

**if**  $\alpha_e^{1/2} - \alpha_\ell^{1/2} > \delta$  **or**  $\ell \in S_\tau$  **then**  
| Set  $e = \ell$ ,  $i_e = i_e + 1$  and  $\tau_{i_e} = \ell$ .

Set  $\tau_R = 1000$ .

---

Additional plots. We now proceed to illustrate the first 2 components for one of the measurement models for all the different combinations of DDIM steps and  $(d_x, d_y)$  combinations used in table 1. Figures 5 and 7 and ?? are grouped by  $d_y = 1, 2, 4$  respectively.

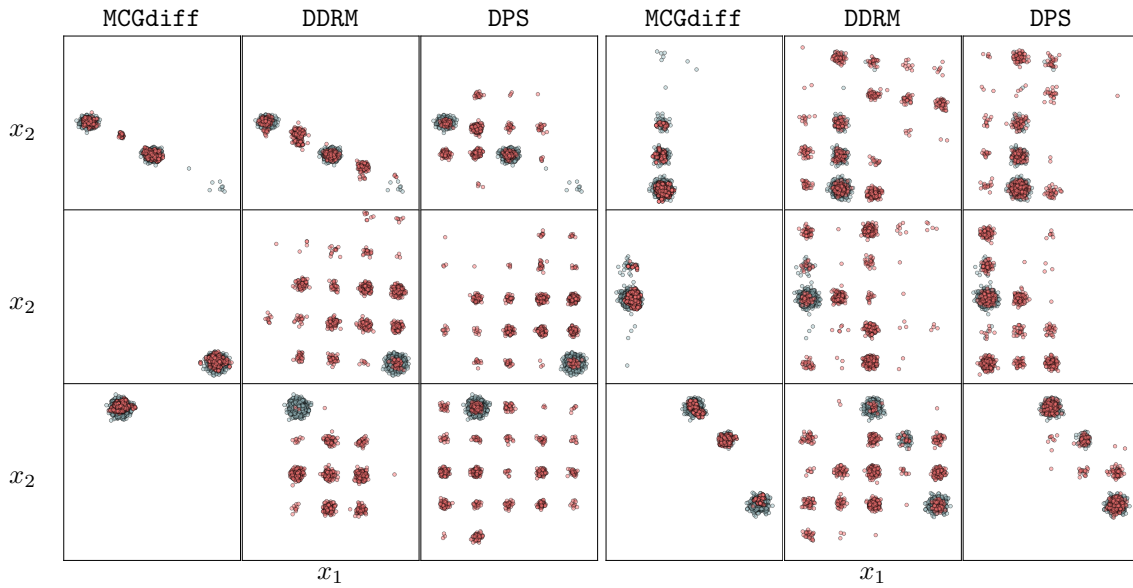


FIGURE 5. We display the first two dimensions of the GMM inverse problem for one of the measurement models tested. The blue dots represent samples from the exact posterior, while the red dots correspond to samples generated by each of the algorithms used (the names of the algorithms are given at the top of each column). The first three columns correspond to 20 DDIM steps and the last three to 100 DDIM steps.  $d_y = 1$  and  $d_x = (8, 80, 800)$  from top to bottom.

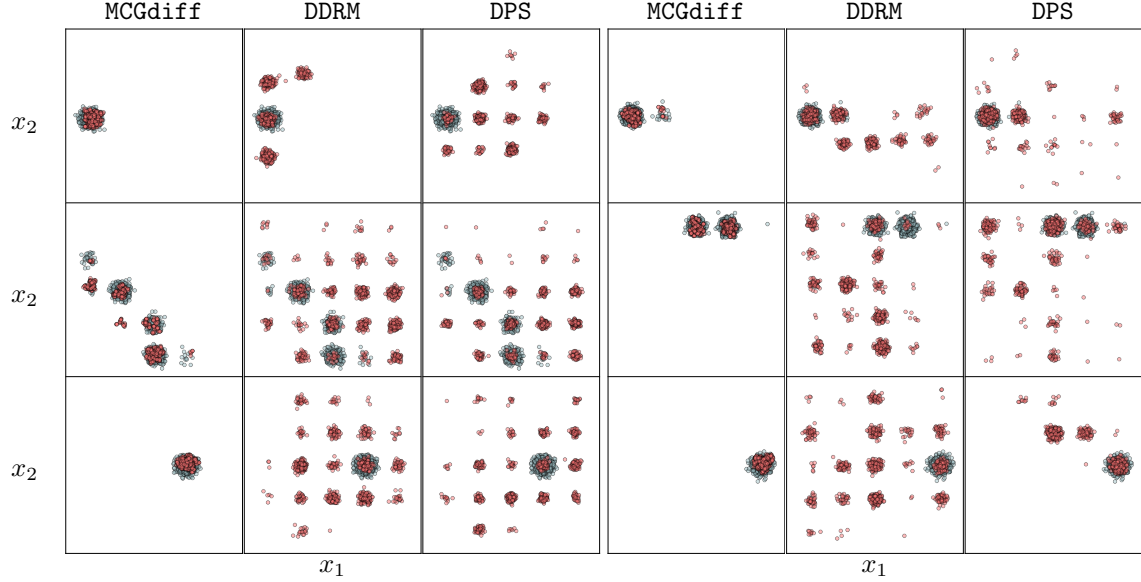


FIGURE 6. We display the first two dimensions of the GMM inverse problem for one of the measurement models tested. The blue dots represent samples from the exact posterior, while the red dots correspond to samples generated by each of the algorithms used (the names of the algorithms are given at the top of each column). The first three columns correspond to 20 DDIM steps and the last three to 100 DDIM steps.  $d_y = 2$  and  $d_x = (8, 80, 800)$  from top to bottom.

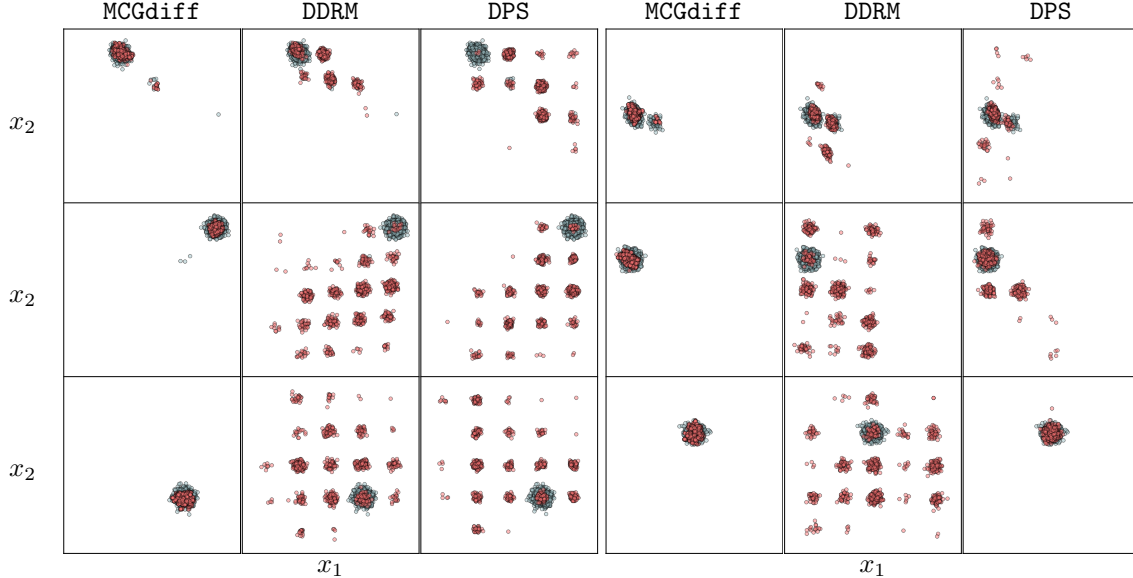


FIGURE 7. We display the first two dimensions of the GMM inverse problem for one of the measurement models tested. The blue dots represent samples from the exact posterior, while the red dots correspond to samples generated by each of the algorithms used (the names of the algorithms are given at the top of each column). The first three columns correspond to 20 DDIM steps and the last three to 100 DDIM steps.  $d_y = 4$  and  $d_x = (8, 80, 800)$  from top to bottom.

We also show in fig. 8 the evolution of each observed coordinate in the noise case with  $d_y = 4$ . We can see that it follows closely the forward path of the diffused observations indicated by the blue line.

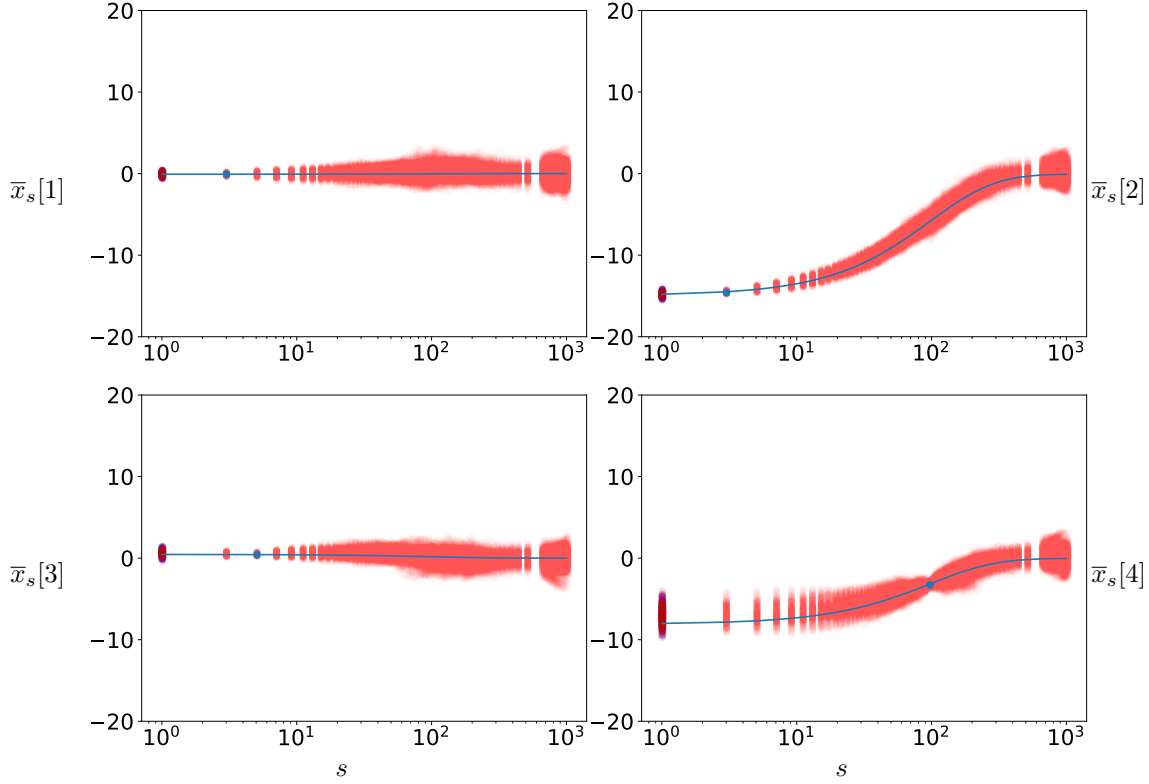


FIGURE 8. Illustration of the particle cloud of the 4 first observed coordinate in the case  $(d_y, d_x) = (4, 800)$  with 100 DDIM steps. The red points represent the particle cloud, while the purple points at the origin represent the posterior distribution. The blue curve corresponds to the curve  $s \rightarrow \alpha_s^{1/2} \mathbf{y}[\ell]$  and the blue dot on the curve to  $\alpha_{\tau_\ell}^{1/2} \mathbf{y}[\ell]$ .

B.3.2. *CelebA*. We show in fig. 9 the evolution of the particle cloud with  $s$ .

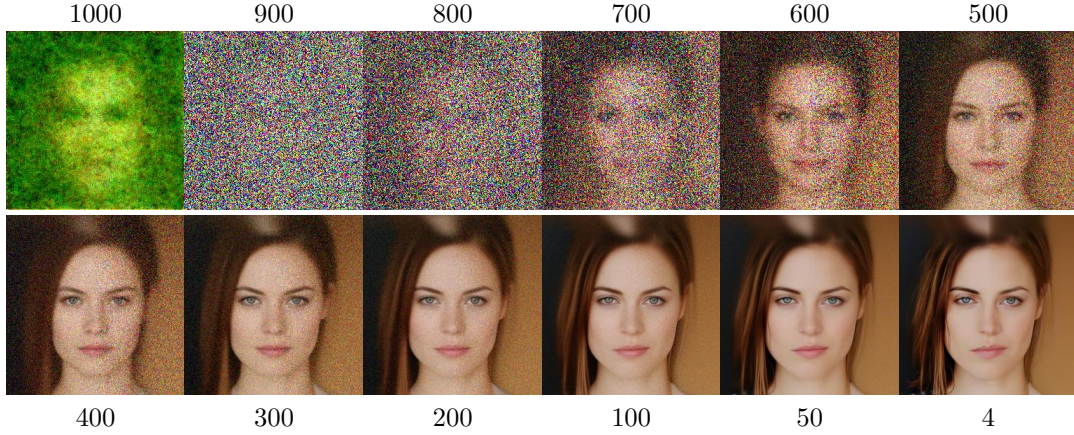


FIGURE 9. Evolution of the particle cloud for one of the masks. The numbers on top and bottom indicate the step  $s$  of the approximation.